This is to certify that the
thesis entitled

Aeration by Water Assisted Micro-bubble Generation

presented by

Mulyanto W. Poort

has been accepted towards fulfillment
of the requirements for the

Masters degree in Mechanical Engineering

Major Professor's Signature

December 7th 2004

Date

AERATION BY WATER-ASSISTED MICRO-BUBBLE GENERATION

By

Mulyanto W. Poort

A THESIS

Submitted to
Michigan State University
In partial fulfillment of the requirements
for the degree of

MASTER OF SCIENCE

Department of Mechanical Engineering

2004

ABSTRACT

AERATION BY WATER-ASSISTED MICRO-BUBBLE GENERATION

By

Mulyanto W. Poort

The main goal of this project was to evaluate the application of a newly found micro-bubble generation technique to water aeration. The micro-bubble generation technique is a water-assisted method where a thin air stream, surrounded by a water stream that flows through an orifice is broken up into bubbles between 100 and 500 microns in diameter. The main advantage of this technique is that it eliminates any solid-gas surface free energy forces, which prohibit the "cheap" generation of micro-bubbles in today's aerators.

The project primarily consisted of designing, building and evaluating the performance of prototypes and testing them for stable operation. The prototypes were submerged in a test tank and evaluated on their ability to produce micro-bubbles, and later, on their ability to aerate.

Through experimenting with a first set of "single-stream" prototypes, it was found that this technique in its original working was unpractical even though it produced very good aeration efficiencies. Having demonstrated the aeration capabilities of single-stream prototypes, multi-stream prototypes were built and tested and it was found that their aeration capability was acceptable though their efficiency was much lower. Standard Aeration Efficiencies ranging between 3.00 and 6.00 lb/hp·hr were achieved. It is expected that the Standard Aeration Efficiency can be improved, as with almost all diffuser aerators, by submerging the aerator deeper under water.

ACKNOWLEDGEMENTS

It has been a true fortune to have had this opportunity to continue my studies and be involved in this research. Foremost, I would like to extend my sincere thanks to my advisor Dr. Giles Brereton for giving me the opportunity to work on this project. I came to work in his lab for a summer job, and the result, this thesis, is more than I could have hoped for. My appreciation goes out to my other committee members Dr. Brian Thompson and Dr. Craig Somerton who were also a very positive guidance during my undergraduate studies. Furthermore, I would like to thank the people at the Engines Research Lab for their help and support on this project and making an unfamiliar place familiar especially Josh Bedford and Tom Stuecken, who patiently worked on many of the prototypes presented in this thesis. I would also like to thank Anna Graf and my brother, Maarten Poort, who worked on this project before my arrival. And lastly I would like to thank my family, especially my parents, Henny and Tilly, my brothers and Jessica for their love, support and encouragement.

TABLE OF CONTENTS

LIST OF TABLES

LIST OF FIGURES

Note: Images in this thesis are presented in color.

LIST OF SYMBOLS AND ABBREVIATIONS

Symbol	Description
BOD	biological oxygen demand
C	concentration
cm	centimeter
d	diameter
D	diameter
$\mathcal{D}$	diffusivity
DO	dissolved oxygen
g	gram, gravitational acceleration constant
hp	horsepower
hr	hour
K	degrees Kelvin
K_a	total mass transfer coefficient
kg	kilogram
k_L	mass transfer coefficient
kPa	kilopascal
kW	kilowatt
l	liter
lb	pound
$\dot{m}$	mass flow rate
m	meter
max	maximum
mg	milligram
min	minimum, minute
ml	milliliter
mm	millimeter
OTE	oxygen transfer efficiency
OTR	oxygen transfer rate
P	pressure
Pa	pascal
Psi	pounds per square inch
r	radius
R	universal gas constant
R_P	pressure ratio
R_Q	flow rate ratio
Re	Reynolds number
Q	volume flow rate
s	second
SAE	standard aeration efficiency
Sc	Schmidt number
Sh	Sherwood number
SOTR	standard oxygen transfer rate
t	time

T	temperature
u	velocity
V	volt
$\forall$	volume
W	watt, work

Subscripts

a	air
i	inner
o	orifice, outer
w	water
∞	saturation

Greek

η	efficiency
μ	micron
Ω	formation rate
π	constant, 3.14...
ρ	density

CHAPTER 1

INTRODUCTION

1.1 Motivation

Aeration of water occurs in many situations. Municipal water treatment plants, private industrial wastewater treatment plants, fish farms, aquariums, lagoons [1] and even natural lake and river systems are aerated. The main reason for aeration is the elimination of unnatural and hazardous chemicals in the water and the improvement of water quality and oxygen levels for a healthy environmentally safe aquatic system. One of the major water treatment operations is the maintaining or increasing the dissolved oxygen (DO) level to an accepted environmentally friendly percentage. Today, several aeration/oxygenation techniques are used to infuse the DO-depleted water with oxygen. However, these techniques can be very energy inefficient and lead to expensive operating costs of the aeration systems.

The most common aeration technique is aeration through diffusion by the under-water release of air (or oxygen). Instinctively, it can be concluded that, for the same amount of air released, if more oxygen diffuses to the water before it reaches the water surface, the subsequent aeration is more efficient. Mass transfer laws then determine that the greatest air-water interface surface area results in the highest transfer of oxygen. Thus, the most efficient diffusion aerator (or *diffuser*) is what the industry terms *a fine-bubble diffuser*: an aerator that produces very small bubbles. Today's typical fine-bubble diffusers are either ceramic discs with micro-pores operating at relatively high pressures or another perforated medium (e.g. plastics) operating at lower pressures.

In an attempt to improve on the current designs, a potentially more efficient fine-bubble (or *micro-bubble*) generator was developed based on the micro-bubble generation technique pioneered by Spanish scientists Gañán-Calvo and Gordillo [2] which utilized the focusing of co-flowing fluids (air and water-ethanol) to generate micro-bubbles. If successful the development of the equivalent air-water micro-bubble generator should, primarily, create an aerator that:

- Is more energy (cost) efficient than existing aerators
- Has similar total aeration capability as existing aerators
- Has a similar compactness as existing aerators

The long-term goal of the project is to create a self-sufficient aeration unit powered by alternative energy sources. Most practical, for now, would be the use of solar energy to power the aerator.

1.2 Introduction to aeration and mass transfer from micro-bubbles

To evaluate an aerator's aeration power it should be tested under stable conditions. The amount of oxygen transferred to the water can be calculated from the change in oxygen concentration of the water. Because mass transfer is a first-order rate process, the equation for the total aeration by an aerator can be expressed in the following differential form:

$$\frac{dC(t)}{dt} = K_a\left(C_\infty - C(t)\right),\ C(0) = C_0,\ C(t \to \infty) = C_\infty \tag{1}$$

leading to the solution:

$$\frac{C(t) - C_\infty}{C_0 - C_\infty} = e^{-K_a(t - t_0)} \tag{2}$$

The concentration difference C_∞-$C(t)$ is the diffusive driving force [3]. A larger difference increases the rate of the process, while a smaller difference decreases it. The diffusive driving force can be improved by increasing the saturation concentration of the water. This can be achieved by increasing the partial pressure of oxygen in the gas or increasing the pressure of the system. However, in large-scale aeration, this is not practical.

The oxygen concentration $C(t)$ is usually expressed as a mass fraction such as mg/kg, ppm or mg/L where the density of water is assumed to be constant. The saturation concentration C_∞ depends on the water temperature and purity (salinity) but usually ranges between 7 and 11 mg/L. For tap water at room temperature the saturation concentration is very close to 9.00 mg/l. Contaminants in the water may reduce the saturation level to as low as 6 mg/l for warm water.

In (1) and (2), K_a is the total aeration coefficient of the aerator in units of 1/s. The value of K_a is characteristic to the aerator and its operating conditions. It is affected by various operating conditions and most significantly by the total water-air interface area and the submersion depth (the time the bubbles are in the water). In a homogenous process (e.g. uniform concentration, temperature, etc.), K_a can be divided into the sum of K_as each representing one, or a group of bubbles. Later on, it will be shown that each bubble can be given a characteristic oxygen transfer coefficient k_L. In that case, K_a can be expressed as a function of each bubble's k_L and it's various other attributes (e.g. bubble size, shape, time in the water, etc.).

The value of the total aeration coefficient K_a can be calculated theoretically using equations of state and mass transfer models when the exact bubble diameters, bubble

number, release depth, operating pressures and temperatures are known. However, in a case with multiple bubbles, even numerical solutions are virtually impossible to obtain due to the large number of bubbles in close random proximity of each other, the reduction in size of the bubbles as mass is transferred to the water, the compressibility of the gas within the bubbles and the impurities in both the liquid (water) and gas (air).

Although an exact theoretical value for the total aeration coefficient cannot be obtained, the experimental value of the total aeration coefficient can be easily found by knowing the saturation concentration and at least two concentrations measurements with their respective time value. Evidently, K_a can be approximated by measuring the change in concentration over time by solving for equation (2).

$$K_a = \ln\left(\left(\frac{C_1 - C_\infty}{C_0 - C_\infty}\right)^{-1/(t_1 - t_0)}\right) \approx \frac{C_1 - C_0}{C_\infty - C_{avg}}\left(\frac{1}{t_1 - t_0}\right) \text{ as } \Delta t \to 0 \tag{3}$$

In analyses of experimental data, this approximation will be used extensively, since, the experimental values for C_0, C_1, C_{avg}, C_∞, t_1 and t_0 can be easily obtained or are known.

Experiments performed during the last 30 years showed that the same volume broken up into very small bubbles transfers oxygen faster solely through the increase of surface area [4]. The mass transfer rate (k_L) of oxygen between an air bubble and water can be expressed as a function of experimentally obtainable values [5]:

$$k_L = \frac{H\left(d_0 + d_f\right)}{12RT\Delta t} \ln \frac{P_0 V_0}{P_f V_f} \tag{4}$$

From (4), the mass transfer rate per unit area (mass transfer coefficient k_L) is dependent on the varying factors of: diameter (d), pressure (P) and volume (V). H is the Henry's law

constant (HLC) and is, in the strictest sense not a constant as it is characteristic of each solute-solvent combination and it varies with temperature. The Henry's law constant can be expressed in units of concentration/concentration where the constant is denoted as H_{cc}, mole fraction/mole fraction or H_{xy}, partial pressure/mole fraction or H_{px}, or partial pressure/concentration or H_{pc} [6]. Here the units for HLC are kpa-m^3/kmol and $H=H_{pc}$.

Table 1. Mass transfer correlation from literature for forced convection from small spheres.

Source	Validity Range	Correlation	Analysis
Frossling	-	$Sh = 0.6Re^{0.5}Sc^{0.33}$	$k_L \approx 0.01$ cm/s
Williams	$4 \leq Re \leq 400$	$Sh = 1.5Re^{0.35}Sc^{0.33}$	$0.01 \leq k_L \leq 0.03$ cm/s
Calderbank & Korchinski	$1 \leq Re \leq 200$	$Sh = 0.43Re^{0.56}Sc^{0.33}$	$k_L \leq 0.01$ cm/s
Barker & Treybal	-	$Sh = 0.02Re^{0.833}Sc^{0.5}$	$k_L \leq 0.007$ cm/s
Griffith	$Re > 1$	$Sh = 2 + 0.57Re^{0.5}Sc^{0.35}$	$0.01 \leq k_L \leq 0.02$ cm/s
Calderbank & Moo-Young	-	$k_L = 0.31Sc^{-2/3}\left(\frac{(\Delta\rho)\mu g}{\rho^2}\right)$	$k_L \approx 0.01$ cm/s
Ahmed & Semmens	$0.01 \leq Re \leq 100$	$Sh = 0.4911Re^{0.3824}Sc^{0.33}$	-
Motarjemi & Jameson	-	-	$k_L \leq 0.05$ cm/s

Adapted from [7], $Sh=k_L r/D$

Studies performed by Motarjemi and Jameson, and Pasveer [5] concluded that the actual transfer rate of oxygen per unit area across the gas-liquid interface decreases for smaller bubbles as the interface becomes immobile. This notion, however, is challenged by various different experiments (Table 1). Empirically, these experiments concluded that the value of k_L might indeed changes with the increase of the bubble diameter [7], but the results showed slightly different trends and most showed minimal variance in the value for k_L.

Although individual experimental results are not in exact agreement, the results primarily show that the value of k_L is approximately 100 micron/s. Only Motarjemi and Jameson found that increased bubble size resulted in a slight increase in k_L, while the first six entries in Table 1 found little variance in the value of k_L. The values for k_L are the normalized mass transfer coefficient and should not be confused with K_a, the total mass transfer coefficient for an aerator. However, the correlation between bubble size and their mass transfer coefficient is consistent with the notion that smaller bubbles improve oxygen transfer efficiency of aerators.

Because in bubble aeration so many bubbles are formed, these single-bubble experiments can be used merely as guidelines. Factors such as coalescing, mixing and water quality greatly affect the aeration process. The overall effectiveness and efficiency of an aerator is then expressed by three numbers:

- Standard Oxygen Transfer Rate (SOTR): quantifies the total amount of oxygen transferred (mass) per unit of time. Naturally, a very large aerator would have a much higher SOTR than one of smaller size.

$$SOTR = K_a V C_\infty \tag{5}$$

- Standard Aeration Efficiency (SAE): quantifies the energy efficiency of the aeration. It divides the total oxygen transferred (mass) by the energy input. It is still somewhat ambiguous what number to use for energy input, whether to use the shaft power (brake power) [8] or the electrical power (wire power). For practical purposes it is best to express the SAE in terms of the rated power of the aerator [9]. For the cases represented in this project, the SAE is

expressed in terms of the pumping work input and can subsequently be multiplied by the pumping efficiency to obtain the SAE in terms of rated power, and the wire to shaft efficiency to obtain the SAE in terms of the electrical power. Since the experiments did not attempt to find the most energy efficient pumps and electrical motors, no attempt was made to express the SAE in terms of rated or wire power.

$$SAE = \frac{SOTR}{\dot{W}_{in}} = \frac{K_a \forall C_\infty}{\dot{W}_{in}} \tag{6}$$

- Oxygen Transfer Efficiency (OTE): quantifies the fraction of oxygen that is transferred to the water compared to the total amount of oxygen that is passed through the aerator.

$$OTE = \frac{\dot{m}_{oxygen,transferred}}{\dot{m}_{oxygen,pumped}} = \frac{\frac{dC}{dt}\forall}{\dot{m}_{oxygen}} \tag{7}$$

Both SAE and SOTR are adjusted to the water condition and express the described quantities as if the oxygen content of the water is zero and the oxygen saturation level is at a standardized value. In this manner every aerator can be rated under the same theoretical standardized conditions. In certain specific areas of oxygenation research, where the efficiency of an aerator may vary under different oxygen content and saturation levels, these two values may be inadequate to practically quantify an aerator's performance. For the research presented in this report, both SAE and SOTR are very

good indicators for the aerator's performance and will be referred to extensively. OTE, as later described, can be an important indicator of an aerator's bubble size.

Having found that the same volume divided into smaller bubbles increases oxygen transfer due to the larger surface area, attention will now be given to the interpretation of units and the method for creating these smaller bubbles.

1.3 Interpretation of units

In this report several different values for SAE and SOTR are presented. It is common for industry to rate SAE in terms of lb/hp-hr. Typical aerators may have SAE values between 1 and 4 lb/hp-hr. This report will report SAE in lb/hp-hr for comparison reasons. SAE may also be expressed in units of kg/kJ or kg/kW-hr. Note that kg/kW-hr and lb/hp-hr are of the same order.

On the other hand, SOTR is best expressed in mg/s because concentrations are given in mg/l and time is given in seconds. For comparative reasons SOTR may be expressed in lb/hr. However, since the aeration capacity of the prototypes tested in this project is fairly small the unit mg/hr is preferred. The preference for units is related to the order of the value, which is preferably of order 1 or 10. To summarize, the following is a table of preferred units that are used in this report:

Table 2. preferred units and value ranges

	Preferred Units	Value Range in Preferred Units	Other Units
SAE	lb/hp-hr	1 - 100	kg/kW-hr, kg/kJ
Overall SOTR/OTR	mg/hr	10 - 1000	mg/s, lb/hr
Per needle SOTR/OTR	mg/hr	10 - 100	mg/s, lb/hr
OTE	percent	10 - 100	fraction
Biological Oxygen Demand	mg/l	1 - 100	ppm, kg/kg
Concentration	mg/l	0.1 - 10	ppm, kg/kg
Mass transfer coefficient	1/s	10E-7 - 10E-5	1/hr

1.4 Introduction to micro-bubble generation techniques

Recent experiments performed at the University of Sevilla showed a liquid assisted method of micro-bubble generation involving co-flowing fluids (water-ethanol and air) through a micro orifice. Not only did this technique generate micro-bubbles but it also created them at constant intervals and in equal size. This so called monodispersed-monosize micro-bubble generation has as its primary advantage the ability to create perfectly monosized bubbles within a liquid, which is useful in various manufacturing applications. Its energy efficiency and application to aeration/oxygenation had not been tested.

This micro-bubble generation technique is illustrated in

Figure 1 (rotated 90 degrees). A gas-feeding needle of small diameter (d_n) is positioned within the liquid environment directly beneath a separation plate with an orifice with diameter $d_{orifice}$.

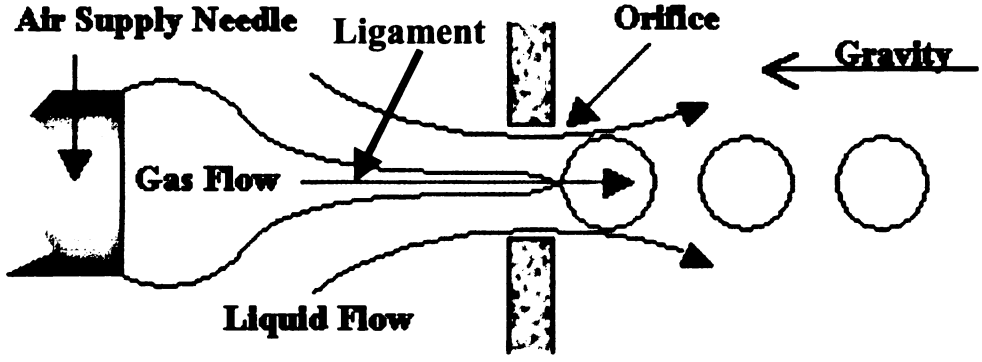

Figure 1. The gas feeding needle is positioned just below the orifice. The nature of the flow is such that a thin gas ligament is formed which subsequently breaks up into micro-bubbles when forced through the orifice.

By increasing the pressure of both the liquid and the gas on the needle-side (or the *upstream* side) of the separation plate, a flow consisting of slower moving liquid on the outside, and a thin fast-moving gas ligament on the inside will converge through the

orifice into the lower pressure region. The nature of the flow is such that the gas ligament will not break up before entering the orifice if the air supply needle is placed close enough to the orifice, but it *will* break up on the other side of the orifice as it is being propelled by buoyancy and the momentum of the liquid flow, thus preventing coalescing of successive forming bubbles. Furthermore, the momentum of the liquid flow ensures that no bubbles make contact with any solid part of the setup, thus preventing "sticking" and bubble growth. To prevent "fusing" or coalescing of bubbles, flow momentum needs to be maintained. The flow rate of the water is therefore very important.

Since the gas flow rate is usually much smaller than the water flow rate, it seems that this bubble generation technique may be a very inefficient method of propelling gas. Thus, it seems that the only advantage of this technique is the small size of the bubbles generated. In fact, using empirical data an equation can be obtained that describes the size of the bubbles generated as a function of the flow ratio of gas and liquid and the diameter of the orifice. Gañán-Calvo and Gordillo found this to be [10]:

$$D_{bubble} = D_{orifice}\left(\frac{Q_{air}}{Q_{water}}\right)^{0.37} \qquad \text{Eq. (8)}$$

Because of the large water to air ratio required to obtain relatively small bubbles, it seems that energy is 'wasted' as far as propelling the air is concerned. It is therefore desired that the water flow rate is minimized while, concurrently, the bubble diameter is kept sufficiently small. A balanced solution should be found, weighing the different parameters, to find a most energy efficient, yet practical, application for this micro-bubble generation technique to the problem.

A theoretical and numerical validation to this technique was presented in [2] by modeling the described coaxial flow of fluids as a linearized model, applying a Blasius-like solution to the liquid-gas interface boundary layer and applying a pressure perturbation at the origin. By observing the behavior of the model at the point of perturbation it was found that the introduced instability was in fact absolute and was not convected downstream, thus explaining the underlying principle of the fixed self-excitation frequency mechanism or *mono-dispersity* of the generated bubbles [2].

1.5 Current bubble aerators

Current aerators that utilize the sub-surface release of air are also called diffusers (Figure 2). Those creating small bubbles (1 to 2 mm) are rated fine bubble diffusers [11] and are usually used to treat aquaculture water. The fine bubble diffusers operate by forcing air through a perforated surface while submerged in water. Air flowing through the small holes will form bubbles and diffuse oxygen to the water as they rise up towards the water surface. The main cause of inefficiency in these aerators is that the bubbles produced are much greater than the holes that create them. For example, ceramic fine-bubble diffusers may have holes that are less than a few microns in diameter, while the bubbles they create are on average 100 micron in diameter, a very inefficient ratio of 1:100. Forcing air through holes this small requires the air to be compressed to a high pressure.

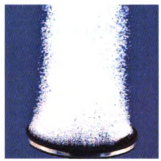

Figure 2. The diffuser aerator utilizes a porous medium to break up the airflow into "small" bubbles, which are then released sub-aquatically and allowed to rise to the surface.

There is a clear correlation between bubble size and required pressure (work) input. The goal is then to find a practical material with the right surface energy to reduce the bubble size without reducing the pore (hole) diameter through which the air travels. Deeper submerged aerators allow for longer rise times of the bubbles before they reach the surface, therefore increasing the amount of oxygen transferred from the bubbles. On the other hand, the hydrostatic pressure is much higher at greater depth, increasing the required work input to the aerator.

Other lesser-used aerators include paddle-wheel aerators, (venturi) injectors, aspirators and propeller aerators. High maintenance and/or aeration efficiency are two reasonswhy these methods are not as common as diffuser type aerators. Of course, certain applications may warrant the use of one of these alternative aerators, mostly where energy efficiency is not important.

CHAPTER 2

EXPERIMENTAL EQUIPMENT

A series of experiments were carried out in large water tanks to measure the efficiencies and transfer rates of prototype aerators. The equipment used is described in this chapter and shown below:

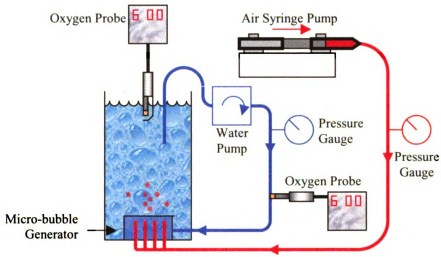

Figure 3. Setup used in several experiments

2.1 Thermo Orion A830 and A862 dissolved oxygen sensors

To measure the dissolved oxygen in water, two Thermo-Orion dissolved-oxygen sensors were used. The more rugged, less versatile A830 had limited application because it requires water flow to prevent depletion of oxygen near the sensor membrane. Two methods that were used to prevent this stratification were: to use a magnetic stirrer to measure a limited sample or to use a pump to create localized water motion. The A862 probe utilized a build-in stirrer to create localized water velocity near the sensor membrane.

Figure 4. Dissolved oxygen sensors from Thermo-Orion used in the experiment. The left probe is the more "rugged" A830 but lacks a stirrer. The right one shows the "more versatile" A862 with a servomotor stirrer to maintain a more steady and accurate oxygen level at the probe membrane.

2.2 Harvard PHD2000 syringe pumps and syringes

Two versions of the PHD2000 syringe pump were used: a self re-filling/dual syringe version that allowed for indefinite and continuous pumping of liquids and a regular single-syringe pump utilizing a 60 ml luer-tip syringe which had to be reset after every 60 ml pump cycle. The theoretical accuracy of these pumps was less than 10 nanoliter/sec. The practical accuracy was about 1-5 µl/min for a pumping rate of 50 µl/min. The dimensions and working of the syringe come into play when performing very precise pumping operations. Practically, the pump is only as accurate as the syringe. Since the pumping rates required were between 0.1 and 20 ml/min, and averaged accuracy was not as important, plastic medical syringes were used (1, 5, 20 and 60 ml).

Figure 5. Harvard PHD2000 syringe pump

2.3 Nikon D100 camera

This versatile 6.1 megapixel camera was used to photograph micro-bubbles suspended in water. The shutter speed range of 1 to 1/4000 second was excellent for capturing relatively fast moving bubbles without blurring. The small aperture required, however, reduced the focus range significantly producing a more 2D-like picture. For photographing micro-bubbles diffused backlight flash was used, essentially "freezing" the picture at speeds much faster than those attainable with shutter control.

Figure 6. The Nikon D100 camera used for photographing micro-bubbles.

2.4 Olympus SZX9 stereo zoom microscope with OLY-200 video camera

This 6.3×-57× microscope (effectively 1200× on 25 inch monitor) was used to inspect apparatus machining jobs for dimension and accuracy. It was primarily used to measure the cleanliness and dimensions of the micro-bubble generator orifice. The microscope was used in conjunction with a camera which could display the magnified image on any television screen.

Figure 7. The Olympus Stereo Zoom microscope used for inspecting the finer details of the aerator.

2.5 Little Giant submersible water pumps

Two submersible pumps were used to provide water flow for the multi-stream prototypes. The pump that was mainly used was a 1/40 hp, 300 gph pump. The other was a 1/125 hp, 170 gph pump. The power of the 1/40 sufficed for use in prototypes with 25+ streams and provided adequate head for the application. The efficiencies of these pumps were low, and they were operated at a low point on their efficiency curve.

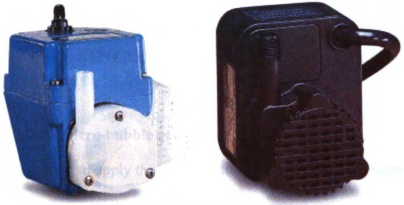

Figure 8. 1/40 hp pump (left) and 1/125 hp pump (right)

2.6 Other equipment

Other equipment that was used included a weight scale from which to infer the mass flow rates of prototypes. Various pressure gauges were used to measure operating pressures. General workshop tools were used to make the prototypes. Tools that were used include:

- High speed micro drill press
- Drill press
- Lathe

CHAPTER 3

MICRO-BUBBLE GENERATION: STABILITY AND REPEATABILITY

3.1 Introduction to micro-bubble generation repeatability

When attempting to apply the aforementioned micro-bubble generation technique to the problem of water aeration, several initial development steps were taken to explore its repeatability and applicability. Questions to be answered included: can the micro-bubble generation technique be reproduced using simple building materials and tools? Can it be reproduced in a less-controlled environment? Although the experimental setup seems simple, Gañán-Calvo and Gordillo recognized the difficulties encountered in this micro-bubble generation technique and questioned its practicality [12]. To evaluate this practicality, several experimental setups were explored to find suitable operating conditions and dimensions for subsequent prototypes. While several aerator prototypes were tested and found successful (they produced a steady supply of micro-bubbles), their aeration capabilities were also measured, and their aeration efficiencies calculated. Since these prototypes created a single stream of bubbles from a single needle and orifice, they were labeled "single-stream" prototypes.

3.2 Experimental setup

The experimental setup consisted of two distinct parts: the fluid feeding and measuring setup and the aerator setup. The fluid feeding and measuring setup (Figure 9) was rarely changed and consisted of water and air supply pumps, a hydrostatic pressure reservoir, pressure gauges and oxygen concentration measurement devices. The syringe

pumps allowed for precise feeding of fluids, while the hydrostatic pressure reservoir dampened the flow fluctuations caused by periodic reversal of the syringe pump. The operating pressure could be directly calculated by measuring the difference between water levels in the test tank and the hydrostatic pressure reservoir. The air pressure was expected to be about the same as the water pressure as both water and air flow discharged from the same reservoir. Air pressure was measured independently to validate this hypothesis.

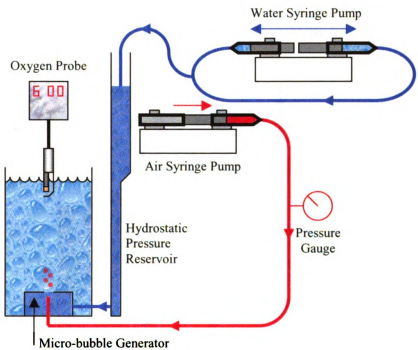

Figure 9. Experimental setup for single-stream experiments.

When a prototype was found to operate successful, its aeration capabilities were measured using a dissolved oxygen probe suspended near the surface of the water in the test tank. A major problem encountered was the affinity of bubbles to the probe's surfaces. Free-rising bubbles tended to accumulate on the probe membrane increasing the perceived oxygen concentration in the water. To solve this problem, a guard was put in

between the probe membrane and the stream of rising bubbles to redirect them around the probe itself. This stopped the direct contact between the rising bubbles and the probe membrane. The guard was designed such that it avoided stratification of oxygen concentration due to the guard blocking the water flow. The goal is to inhibit bubble movement near the oxygen probe, but still encourage flow of water in the area. Although the automatic stirrer attached to the oxygen probe encourages water flow at the membrane area, it does not necessarily create a good "turn-over" of the water in the area. However, leaving enough flow passages perpendicular to the bubble flow but parallel to the water flow caused by the stirrer will easily solve this problem.

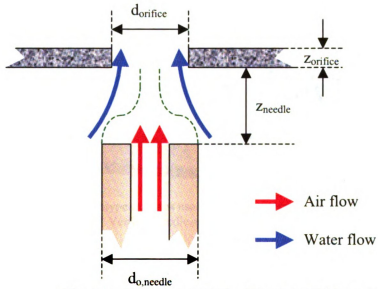

Figure 10. Aerator setup showing important variable parameters.

The aerator setup was changed systematically to find the best micro-bubble generation setup. When considering the experimental setup in Figure 10, several physical parameters were changed, including:

- Orifice diameter
- Orifice height

- Needle inside and outside diameter
- Distance between needle and orifice

Operating parameters, including fluid flow rates and pressures, were also varied in order to observe the effect of those changes.

The first prototype (Figure 11) was created by prior research assistants and was consequently modified to simplify the process of varying physical parameters. Due to the bulk of the prototype, it was replaced by a much smaller one.

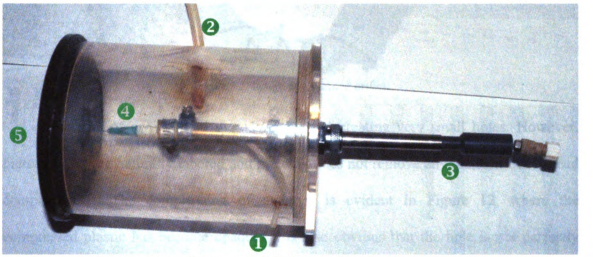

Figure 11. Existing prototype that was used for initial experiments. (1) Air inlet; (2) Water inlet; (3) Vertical needle adjuster; (4) Needle; (5) Orifice.

The second prototype (Figure 13) utilized a small plate with an orifice, clamped between two rigid layers. The plate containing the orifice could be switched with any other plate with different orifice dimensions. Furthermore, the plate could be moved laterally and be positioned in any desired lateral position. The plate containing the orifice was usually a 300μ thick transparency plastic sheet in which the orifice was pierced using one of several pins. Orifice diameters could be pierced to about 150μ diameter. The size of the orifices was measured and validated using the Olympus stereo zoom microscope.

In certain cases, the 300μ transparency plastic was replaced with a 50μ or 100μ aluminum sheet.

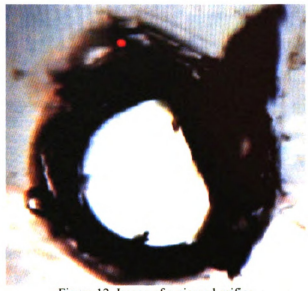

Figure 12. Image of a pierced orifice

Piercing of orifices had the advantages of creating very small holes. However, pierced holes are naturally tapered and piercing does not remove any material but instead compresses it. The compressing of material is evident in Figure 12, where the compressed plastic has become opaque. It is also obvious that the hole is not perfectly round. Drilling the hole, on the other hand, removes a most of material, but the minimum orifice size is reduced significantly to about 250 microns.

The air-feeding needle, being attached to a rubber insert could be moved vertically. Combined with the laterally flexible plate position, the needle tip could be positioned arbitrarily at any position and in any direction below the orifice. Furthermore, the needle modules could be switched so that the prototype could accommodate different sizes of needles.

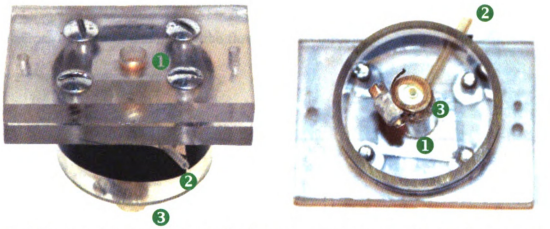

Figure 13. Prototype that enables switching of orifice plates, enabling easy changing of orifice dimensions.

Needle modules (Figure 14) enable the quick switching of different needles into the same prototype. Needle modules consisted of a needle, encased in a rigid body and then inserted into a rubber sleeve (hose) so that when the module is inserted into one of the prototypes it will create an airtight and watertight seal under its operating pressures (<5 psi).

Figure 14. Four different needle modules with different needle dimensions (left) and a needle module inserted into one of the prototypes (right).

The inserted needle module (Figure 15) also creates a water chamber, called the "upstream" section of the aerator, where the pressure is increased to create a pressure drop across the aerator and induce the flow of fluids through the orifice.

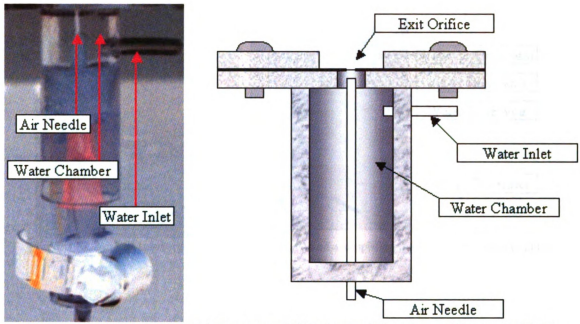

Figure 15. Needle module inserted in prototype (left) and a simplified diagram of the aerator (right).

Needle dimensions varied between 75-750μ inside diameter and 360-2000μ outside diameter. The smaller diameter needles were fused silica tubing, while the larger dimension needles were different sizes of medical syringe needles.

Apart from the varying physical dimensions, all these single stream aerator prototypes were very similar and mainly consisted of: an orifice, a needle, a water inlet and an air inlet. In an attempt to simplify and reduce physical sizes, several smaller prototypes were created. However, their lack of versatility (inability to change certain physical parameters) caused these prototypes to be impractical. These prototypes will not be discussed further.

The aerator setup and the fluid feeding and measuring setup combined to complete the experimental setup (Figure 16). A transparent ruler (or another fixed length

scale) was submerged near the orifice of the aerator for bubble-size measurement purposes. The Nikon D100 camera was used to photograph the bubbles (using diffused backlight flash) with the scale in the background.

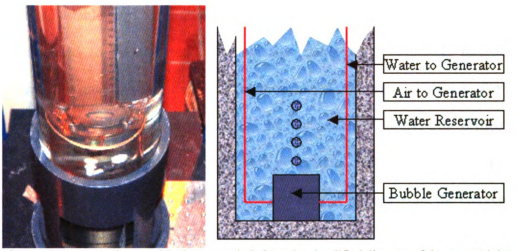

Figure 16. Aerator submerged in the test tank (left) and a simplified diagram of the setup (right).

3.3 Experimental procedure

The experimental procedure is simple but can be lengthy. Firstly, the dissolved oxygen probes are calibrated and polarized. This is done in advance because the calibration and polarization time may take up to an hour. Secondly, the desired flow rates for water and air are programmed into the syringe pumps. Flow rates may range from 0.5-10 ml/min for water and 0.05-2 ml/min for air. The water to air flow ratio varies between 1 and 50, and is essential in calculating the theoretical bubble size.

The fluid lines are then connected to the aerator prototype, and the prototype is submerged in the test tank. While the prototype is submerged the water flow is turned on to flush out any air in the water lines and in the water chamber and to let the hydrostatic pressure reservoir come to steady state. Once the hydrostatic pressure reservoir has

reached steady state (the pressure is such that the flow rate through the aerator orifice is equal to the flow rate from the pump) the air pressure is manually increased to operating pressure and the air syringe pump is turned on.

If no stable and continuous micro-bubble generation is observed, physical parameters need to be changed to obtain this stable and continuous micro-bubble generation. This may involve changing the location of the orifice relative to the needle tip, changing the fluid flow rates or changing the physical dimensions of the orifice.

If stable and continuous micro-bubble generation, with micro-bubbles diameters less than 500μ, is observed, oxygen concentration may be logged using the oxygen probe data logger. This should be done over no less than 45 minutes as transient mixing processes may take several minutes to come to a certain steady state, when oxygen concentration gradients are not due to stratification but due to the aeration process of the rising micro-bubbles.

Bubbles may be photographed against the background of a ruler for bubble size measurements. It is important that the picture is taken at straight angles to the wall surface to minimize refraction. Although the known length scale should solve the major problems caused by refraction, the edge-to-edge difference of length scale in the photograph may still be significant.

The data obtained during the experimental process is then analyzed for trends in oxygenation (aeration) rate and bubble size. Standard Aeration Efficiency and Standard Oxygen Transfer Rate are calculated and compared to industry average numbers for diffuser aerators.

3.4 Results and discussion of single stream aerator experiments

3.4.1 Micro-bubble generation results

Micro-bubbles (Figure 17) were successfully generated using various combinations of geometric and physical setup conditions. However, very few experimental trials could generate micro-bubble continuously for more than two hours. This is a major dilemma as repeatability and reliability is very important for the intended application. The requirement of precise needle positioning seems the biggest problem in creating a reliable device and this will be discussed later. Successful micro-bubble generation required bubble sizes between 0.100 mm and 1.000 mm.

Table 3. Actual observed bubble size versus calculated bubble size from correlation.

	Date				
	19-Nov	3-Dec	4-Dec	4-Feb	12-Feb
Actual average bubble size	200	240	210	400	210
Theoretical bubble size	60	63	79	68	58

It is clear from Table 3 that the actual average bubble size is greater than the bubble size obtained from the correlation discussed in the introduction. This may be due to the fact that the bubbles are photographed downstream from the aerator, where they may have coalesced. This is possible since the experiments utilized high fluid flow rates. In Figure 18, various bubbles with sizes lower than 125 micron can be observed, while some have coalesced into larger bubbles. The measurement of the orifice diameter is imprecise, because of the uneven nature of the orifice (Figure 12). Bubbles could be produced at a slow rate (Figure 17), causing a neat line of bubbles to emerge from the aerator, and at faster rate (Figure 18), randomly dispersing the bubbles as they were formed. It is clear that this random dispersion causes some of the bubbles to merge to

create larger bubbles. The issue of coalescing bubbles and their effect on aeration will be discussed later on.

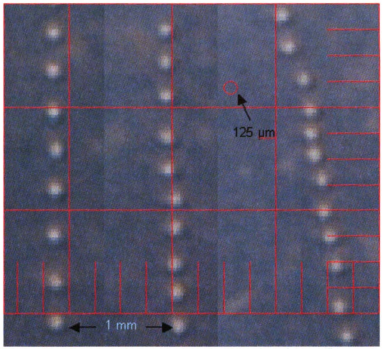

Figure 17. Micro-bubbles generated using low air and water flow rates.

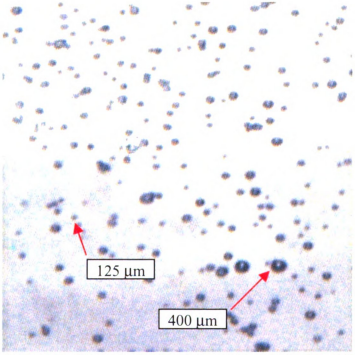

Figure 18. 10 by 10 mm area, bubble sizes range from about 75 to 400 µm

Micro-bubble generation was only considered successful when it was stable and continuous (constant bubble size and amount of bubbles generated over time). Non-continuous micro-bubble generation may be caused by fluctuating pressures and flow rates, clogging of the orifice, or the movement of the needle relative to the orifice.

3.4.2 Aeration results

Oxygen transfer rates were calculated when a steady bubble generation rate was achieved. Table 4 displays selected data for five oxygenation trials. The data assumes an oxygen saturation level of 9.00 mg/l and 100% pump efficiency for the standard aeration efficiency (SAE) and standard oxygen transfer rate (SOTR). For this reason, a practical device would have an SAE of 50%-80% of the values listed in Table 4.

Table 4. SOTR and SAE for three selected experimental oxygenation trials

Date	Average Bubble Diameter (Micron)	Orifice Diameter (micron)	Water Flow Rate (ml/min)	Air Flow Rate (ml/min)	SOTR (mg/hr // lb/hr)	SAE (kg/kW hr // lb/HP hr)
19-Nov	200	100	0.8	0.20	6.86 // 1.51E-5	36.19 // 59.62
3-Dec	240	160	2.5	0.20	6.89 // 1.52E-5	22.49 // 37.06
4-Dec	210	160	2.0	0.30	8.61 // 1.90E-5	31.61 // 52.07
4-Feb	400	160	3.0	0.30	4.33 // 0.96E-5	8.84 // 14.56
12-Feb	210	110	1.8	0.32	8.19 // 1.81E-5	27.85 // 45.88

According to theory, smaller bubbles should increase the oxygen transfer rate at the same air volume flow rate but not in proportion to the total surface area of the bubbles due to the rate of mixing at the small scale, and the density of the bubbles.

3.4.3 Discussion

When continuous and stable micro-bubble generation was achieved the aeration efficiencies that were achieved were very high. The measured SAE was 40 lb/(hp·hr)

(practically 20-30 lb/(hp·hr)) for some experimental trials, which is more than ten times as efficient as the best diffuser aerators. However, there were problems of repeatability. With the means available, it was not possible to always position the needle precisely below the orifice, even for a *single stream* aerator. A practical aerator required at least 1000 of these devices in close proximity of each other. At present, the multiplication of this technique is not practical but may be made practical with very precise manufacturing techniques. Even if this aerator could be manufactured with sufficient precision, these tolerances might deteriorate in the harsh operating conditions present in the aeration application.

Instead of abandoning the idea of using this micro-bubble generation technique, a compromise single-stream aerator design was explored. The new design (Figure 19) increased the orifice diameter and depth and required the air-feeding needle to be protruding *into* the orifice.

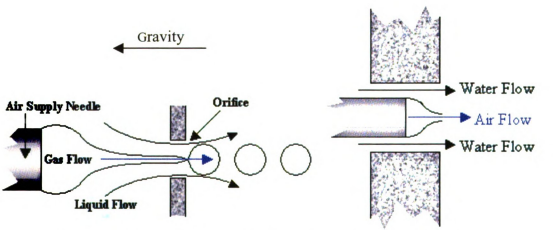

Figure 19. Original aerator setup (left) and new protruding needle setup (right)

This design has some major disadvantages compared to the previous design. If the bubble diameter is a function of the orifice diameter, more water flow, and therefore more energy must be expended to create smaller bubbles. The orifice diameter must be

larger than the needle outside diameter. The smallest needle diameter available is about 200μ in the case of a 100μ ID fused silica capillary tubing. It has been found that the orifice diameter must be at least 500μ in diameter to have a 150μ gap between the needle and the orifice wall for water to flow through. The increased depth of the orifice is also problematic as it increases the pressure drop across the orifice.

For all these efficiency losses, there is one main advantage. The alignment of the needle is automatic in the lateral directions because of its forced protrusion into the orifice. The lateral position is inconsequential, as long as the needle tip is within the orifice cavity.

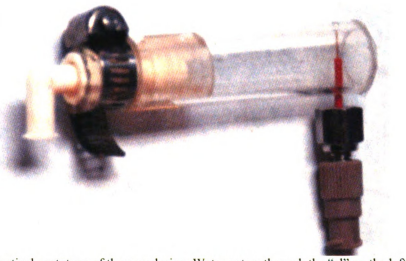

Figure 20. A practical prototype of the new design. Water enters through the "el" on the left while air enters through the union piece attached to a capillary needle. The needle protrudes into the cavity of an orifice drilled through the acrylic tubing wall.

The new design was made into a practical prototype to test for stability in micro-bubble generation but was not tested for aeration capability. It was found that the required air to water flow rate was much higher, while the operating pressure was also a little higher. Since stable and continuous micro-bubble generation was always observed,

it was concluded that, although its efficiency was lower, this design was suitable for implementation into a *multi-stream* aerator prototype.

CHAPTER 4

MULTISTREAM AERATOR DESIGN

4.1 Introduction

With the new needle and orifice design, several theoretical questions were considered before commencing on the multi-stream aerator design:

- What are the changes in the mechanics and dynamics of the fluid flows compared to the original design?
- Where are the major losses in the new design?
- How does bubble generation differ from that in conventional aerators?
- How can the new design be implemented in a multi-stream design?

Since the new design was found to create micro-bubbles continuously, it seemed to work in a similar way to the original design. There are, however, some major differences. From Figure 19, it can be seen that in the original design, an air *ligament* is *focused* through a much smaller orifice. Not only can the orifice be very small, but it also dictates the diameter of the air ligament. Theoretically, the orifice in the original design can be made very small. The advantage of the focusing technique is that the diameter of this ligament can be very small, and the resulting bubbles produced are consequently much smaller too. It can also be noted that a "bulb" shaped bubble attaches to the needle tip from which the ligament rises. This bubble occurs due to the surface energy of the needle. In the new design, this accumulation of air at the tip of the needle also occurs, but

within the orifice itself. Since the air flow is not really "focused" as in the original design, the resulting air *ligament* won't be much smaller in size than the needle diameter itself.

On the other hand, the water flow is highly directional in the new design as it is forced through the gap between the needle and the orifice wall. As the water travels through this gap, its velocity will stay constant and its flow will be parallel to the orifice axis. As the water flows past the needle tip, it has the *ability* to slow down (in the direction parallel to the orifice axis), as the flow is able to move laterally. Downstream from the needle tip, the dynamics of the two designs are very similar, except for the physical dimensions of the orifice and the needle itself.

The major losses in this design are friction losses due to relatively high flow velocities and small flow passages. Theoretical pressure drops were calculated for the major flow losses across the needle, for the air flow, and across the orifice gap for the water flow. Other flow losses were subsequently ignored due to their insignificance compared to those major losses.

Conventional diffuser aerators are not water assisted bubble generators. In conventional aerators, air is simply pumped through very small holes. Here, smaller holes create smaller bubbles, as demonstrated by the following equation [13]:

$$V_{bubble} = \frac{2\pi r_{orifce}\sigma}{g(\rho_{water} - \rho_{air})} \tag{9}$$

Also, the volume of the bubble is linearly proportional to the surface tension. Here the choice of diffuser material becomes very important. The higher free surface energy of the solid material will create more wetting and less surface tension, reducing the bubble size.

In the new design, the free surface energy of the aerator material is inconsequential to the bubble size. Here bubbles aren't created because of the buoyancy

force outweighing the surface tension force, but rather by the instability of a narrow air ligament.

The new design was implemented in a multi-stream prototype. The assembly design called for the use of a standard high-speed micro drill (Ø=500μ), which was used for drilling holes straight through two dividing walls (Figure 21). Needles were inserted, aligned and glued into place.

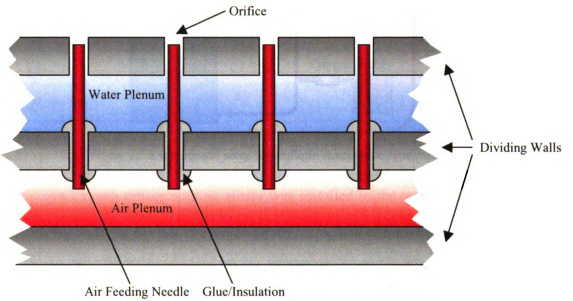

Figure 21. Assembly design for the multi-stream aerator.

The design was then implemented in a practical prototype. Initially prototypes were designed for ease of addition of extra streams, while later prototypes were designed so that they were easy to assemble.

4.2 Experimental setup

The experimental setup for the multiple-stream aerators (Figure 22) is very similar to the one used for the single-stream aerator experiments. The main difference is that a submergible centrifugal pump was used to control the water flow rate. Pressures

were measured using pressure gauges and an oxygen sensor was installed in the water feeding line to the prototype.

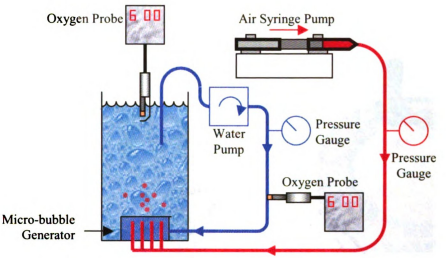

Figure 22. Experimental setup for multiple-stream prototype experiments.

An oxygen sensor with no stirrer was installed in the water feeding line because the moving water in the line prevented stratification and eliminated the need for a stirrer. Air was fed by a syringe pump at rates up to 45 ml/min. Since the water pump output was a fixed 1/40 HP shaft output pump its performance was dictated by the operating pressure of the prototype. Its flow rate could not be adjusted.

In all, seven multiple-stream aerator prototypes were built, six were tested for micro-bubble generation and five were tested for aeration efficiency. The five prototypes are described below:

- The first prototype was machined out of polycarbonate plastic. Polycarbonate was chosen because of its strength and its ability to be machined compared to other plastics, which were insufficiently strong or would melt under high machining speeds. This prototype, being the first multi-stream prototype, only

utilized 10 needles. Its success was marginal, however, as half the needles were obstructed by glue residue and other contaminants before its first operation. This prototype was both tested for micro-bubble generation and aeration capability.

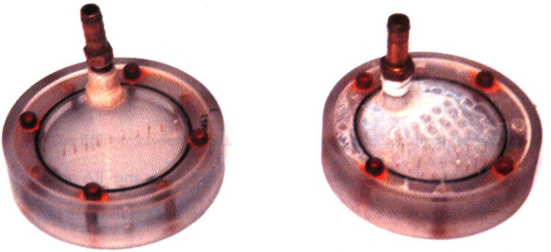

Figure 23. Prototype #1 (left) and prototype #2 (right) showing mineral deposits on the top of the water plenum.

- The second prototype was identical to the first one, but with 40 needles. Again, half the needles were found to be un-operable. This prototype was tested for both micro-bubble generation and aeration capability.
- The third prototype utilized cork as a water and air seal agent. However, it was found that, even with plenty of vacuum grease that this prototype could not be made airtight. This prototype was not tested.
- The fourth prototype was identical to the third one, but instead used a permanent adhesive to seal the air plenum, but still used cork to seal the water plenum. Although some leakage was present, this prototype worked well and was both tested for micro-bubble generation and aeration capabilities

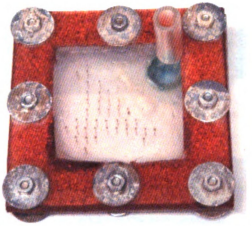

Figure 24. Prototype #4 clearly showing the needles and water inlet. The air inlet is in the back and can be seen through the transparent plastic.

- The fifth prototype was a bar-shaped prototype and arranged the needles in a row. All parts were sealed using a permanent adhesive. It was found that due to the small gap spacing between the needle and the orifice wall, the operating pressure was too high and out of the pump's range. This prototype was tested for micro-bubble generation and failed. The high operating pressure reduced the water flow rate to below what was required for sufficient water momentum. Bubbles of 0.5 to 1.0 mm diameter were observed and were considered insufficiently small to be classified as micro-bubbles.

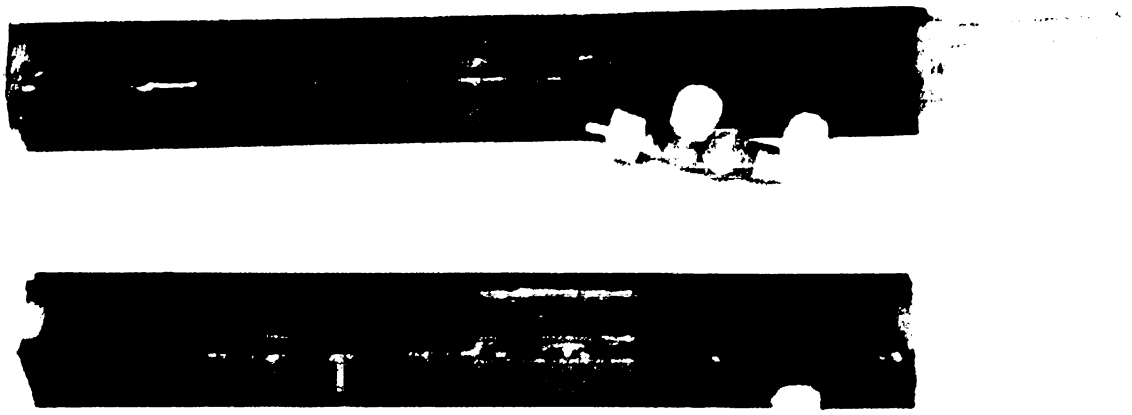

Figure 25. Prototype #5 (bottom) and prototype #6 and #7 (top) which shows the water inlet on the right and the air inlet and check valve on the side

- The sixth prototype was identical to the previous one, except that the gap between the orifice wall and the needle was increased by increasing the orifice diameter from Ø=360μ to Ø=520μ. Also, the needles were aligned flush with the orifice top which had an adverse effect on the bubble size. This prototype was tested for both micro-bubble generation and aeration capability

- The seventh prototype was the same as the sixth, except the needles were reduced in length so that they were recessed below the orifice top as in prototypes 1 to 5. This slightly improved the aeration efficiency of the device. This prototype was tested for both micro-bubble generation and aeration capability

Table 5 shows an overview of the operating properties of each of the five devices tested for aeration capability. All prototypes had orifice diameters of about 500μ-530μ which were made by using a Ø=500μ drill. Prototype seven had an orifice depth of 1.6 mm while all other prototypes listed in the table had an orifice depth of 3 mm.

Table 5. Operating properties of the five devices tested for aeration capability.

Prototype	Needle OD	Needle ID	# Needle	Air Flow		Water Flow		Water/Air	Water/Air
				Total	Per Needle	Total	Per Needle	Designed	Actual
	Micron	Micron	#	ml/min	ml/min	ml/min	ml/min	:	:
#1	360	200	10	20	2.00	500	50	25.0	12.5
#2	360	75	40	45	1.13	1600	40	35.6	14.2
#4	200	100	38	20	0.53	1940	51	97.0	25.5
#6	200	100	35	30	0.86	1410	40	47.0	26.9
#7	200	100	35	40	1.14	1470	42	36.8	21.0

From here on, each prototype might be identified by "# Needle [OD/ID]..." For example: prototype #1 may be identified as "10 Needle [360/200]."

4.3 Experimental procedure

The procedure for testing multiple-stream prototypes is similar to that for single stream prototypes. Once again, the oxygen sensors were calibrated in advance. After calibration, one of the oxygen censors was connected to the water feeding line with its membrane perpendicular to the flow direction. After the prototype was connected to the air and water feeding lines, the water pump was run to flush out any air out of the water supply lines. While the water pump ran, the air supply was brought up to operating pressure to prevent any backflow of water into the air plenum of the aerator prototype. When both the water and air were supplied at their desired rates, the dissolved oxygen concentration was logged using the automatic data logger on the oxygen sensors, with data logging performed over at least 45 minutes.

4.4 Results and discussion

4.4.1 Micro-bubble generation

It was found that for the multi stream prototypes, micro-bubble generation could be achieved continuously. By analyzing the photographs it was found that the micro-bubbles were of sufficiently small size (<500μ).

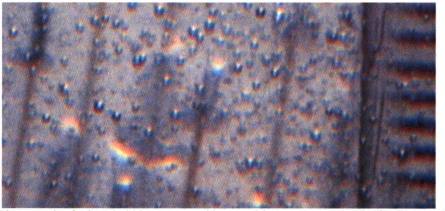

Figure 26. Photograph of micro-bubbles generated by a multi-stream aerator. The feeding needles can be seen as diagonally running lines. For reference, the needle diameter is 200μ.

It is also obvious that not all bubbles are the same size. While some seem smaller than 200μ, others are definitely larger. The lines on the right of the picture may also be used as a measuring reference. The distance between two lines is exactly 1 mm. It is hypothesized that the larger sized bubbles are created due to coalescence right after formation of the bubbles. The bubble formation rate Ω can be easily calculated when the bubble size is known. Considering a per-needle air flow rate of 2 ml/min and a bubble formation diameter of 200μ:

$$\Omega = \frac{2\frac{ml(air)}{min}\cdot 10^{-6}\frac{m^3}{ml}\cdot 0.016667\frac{min}{s}}{\frac{4}{3}\pi\left(0.0001\frac{m}{bubble}\right)^3} \approx 8000\frac{bubbles}{second} \qquad (10)$$

It is worth considering whether this high bubble formation rate is really possible. If the bubbles were packed surface-to-surface when formed, the velocity required for the bubble formation of 200μ would be:

$$u_{bubble} = 8000\frac{bubbles}{second}\cdot 0.0002\frac{m}{bubble} = 1.6\frac{m}{s} \tag{11}$$

This velocity, although it seems small, is rather large for its size. This velocity is also the *minimum* velocity to avoid coalescing at formation. The bubble formation velocity can also be compared to the water velocity at the needle tip to find the *relative* velocity between the bubble and the water at formation. When the per-needle water to air flow ratio is 20, the orifice diameter is 520μ and the needle diameter is 200μ, the average water velocity at the needle tip is:

$$u_{water} = \frac{40\frac{ml(water)}{min}\cdot 0.016667\frac{min}{sec}\cdot 10^{-6}\frac{m^3}{ml}}{\pi\left(260^2-100^2\right)\cdot 10^{-12}\frac{m^2}{\mu^2}} = 3.684\frac{m}{s} \tag{12}$$

When comparing the water velocity to the minimum bubble velocity at formation, it seems possible that this high bubble formation rate can be achieved. Finally, the air velocity at the needle tip can be calculated to calculate the relative velocity of the air to the water at the needle tip. Considering the needle inner diameter is 100μ:

$$u_{air} = \frac{2\frac{ml(air)}{min}\cdot 0.016667\frac{min}{sec}\cdot 10^{-6}\frac{m^3}{ml}}{\pi\left(50^2\right)\mu m^2\cdot 10^{-12}\frac{m^2}{\mu m^2}} = 4.244\frac{m}{s} \tag{13}$$

These numbers clearly show that it is possible for the bubbles to rise at a minimum velocity of 1.6 m/s right after formation. It can be expected that the velocity of the bubbles can be as fast as the relative terminal velocity. The initial bubble velocity can be compared to the Stokes terminal velocity for a rising 200μ micro-bubble of 22 mm/s, or

about 100 bubble diameters per second. The terminal velocity is obviously slower than the velocity at formation, causing the speed of the bubbles to decrease as they rise. It is then not hard to imagine the condensing of space between the micro-bubbles as their rising velocity decreases. Although the bubbles will tend to fan out, coalescing of some of the bubbles is inevitable. This coalescing, in turn, increases bubble size and reduces the total surface area of air-water interface. It is then obvious that this coalescing decreases the aeration efficiency of the aerator.

4.4.2 Aeration capability

As expected, it was found that the multiple-stream aerator, with its new needle positioning, was much less efficient compared to the single stream aerator. While the single-stream aerator had a "perfect pumping efficiency" SAE of over 40 lb/(hp·hr) (Table 4), the multiple-stream aerator SAE (assuming perfect pumping efficiency) was between 2.5 and 5.2 lb/(hp·hr). A higher per-stream SOTR was found. Table 6 shows an overview the performance numbers for each prototype.

Table 6. Performance numbers for the five prototypes tested for aeration capability.

	SAE	SOTR	OTE		Total Water Pressure	
Prototype	Average	Average	Min	Max	Theoretical	Practical
	lb/hp-hr	lb/hr	%	%	kPa	kPa
#1	2.94	0.000439	22.43	47.57	26.02	27.44
#2	4.39	0.001501	61.31	65.88	20.81	24.50
#4	3.75	0.001103	89.24	98.34	6.00	26.46
#6	3.34	0.001237	78.03	92.35	5.02	21.07
#7	4.70	0.001491	58.73	94.38	5.23	19.60

Although Table 6 shows a value for the average SAE and SOTR for each prototype, for some prototypes the performance varied significantly from trial to trial (Figure 27).

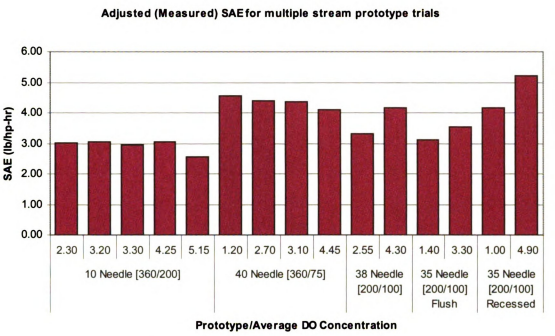

Figure 27. SAE for different trials for each of the five prototypes. (Using C_{∞}=8.75 mg/l)

It is evident that for the first two prototypes the SAE does not change significantly (#1: SAE=3, #2: SAE=4.5) with the average dissolved oxygen concentration. However, the latter three prototypes show an increased SAE for higher average dissolved oxygen concentration. It is hypothesized that this is due to the variation in bubble sizes due to coalescing of bubbles. For lower average dissolved oxygen concentration it is thought that some bubbles (the smallest ones that do not coalesce) are of sufficiently small size that they transfer all their oxygen before reaching the surface. If the same happens for higher dissolved oxygen concentrations (even though the transfer rate is slower), essentially, the same amount of oxygen is transferred to the water but the numbers will show an increased SAE (and SOTR) because of the normalization of the SAE (Figure 28). If the number of this type of bubbles is significant it is expected that the SAE increases for higher dissolved oxygen concentrations.

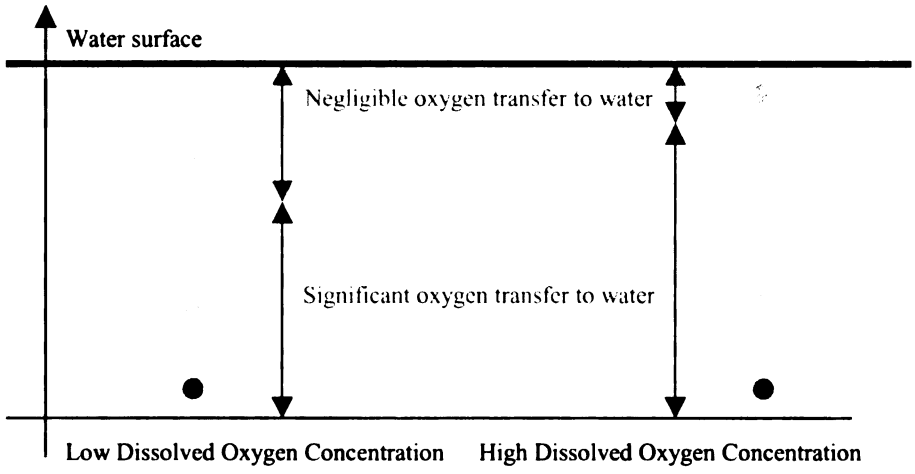

Figure 28. Illustration of complete oxygen transfer to water and effect on SAE. Although in both cases all of the bubble's oxygen is transferred, less (rising) time is required for low DO concentrations. In the end both bubbles have transferred the same amount of oxygen to the water.

Although the new aerator had a higher SOTR, oxygen transfer rates are still the weakness of this water-assisted aerator design. The reason for this is the maximum air flow rate per needle. If the airflow is increased too much the water momentum may not be enough to keep the air from "sticking" to orifice walls. In the experiments, the practical air flow per needle is about 4 ml/min (depending on the prototype, the practical air flow is about double the theoretical flow rate because of clogging of some of the needles). At atmospheric pressure and 293K, the maximum oxygen mass flow would be equal to:

$$\dot{m}_{O_2} = 4\frac{ml(air)}{min}\cdot 10^{-6}\frac{m^3}{ml}\cdot 60\frac{min}{hr}\cdot 1204\frac{g(air)}{m^3}\cdot 0.232\frac{g(o_2)}{g(air)} = 67mg/hr \qquad (14)$$

If we consider the *absolute* operating pressure (~1.25 atm) and assume isothermal compression, the maximum per-needle oxygen mass flow would be closer to 84 mg/hr. Although the air flow rate of 4 ml/min was the maximum air flow tested, it is not necessarily the practical *limit*. This limit was set due to the practical output of the syringe pump and due to results of previous single-stream observations. A higher limit may be

found in subsequent testing. On top of the limited air flow capacity, it must also be taken into account that the OTE (oxygen transfer efficiency: the percentage of oxygen transferred to the water) is rarely 100% (Figure 29).

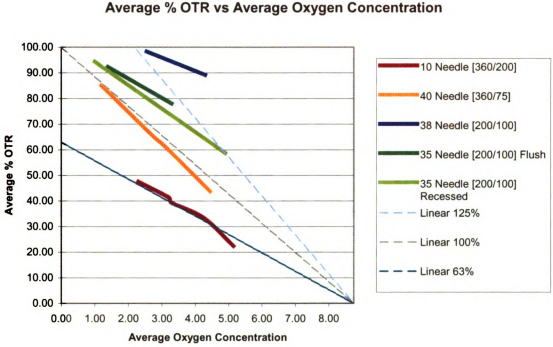

Figure 29. OTE values for each prototype under different DO concentrations.

Although a 100% OTE is possible, it would not necessarily be the most energy efficient operating condition. 100% OTE requires that all oxygen is transferred from the bubbles to the water before they reach the water surface. Since not all bubbles will be the same size, the smaller bubbles will transfer all their oxygen to the surroundings more quickly (Figure 28) and their oxygen will be depleted before they reach the surface. This is inefficient because extra energy was used to make these bubbles so small.

Therefore, a reasonable OTE (from Figure 29) would be about 60%-70% for the latter prototypes. This, of course, would be higher for low DO concentrations and lower for high DO concentrations. The optimum per-needle oxygen transferred would then be

55 mg/hr or 0.000121 lb/hr. This can be compared to the practical SOTR shown in the following figure.

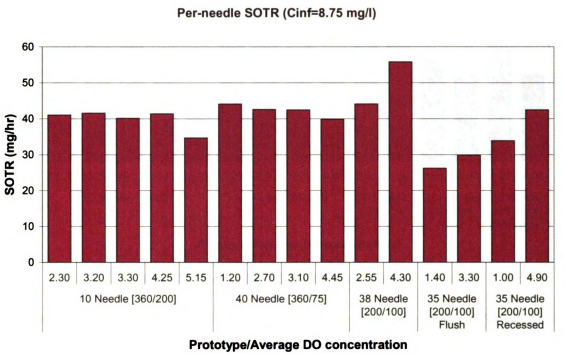

Figure 30. Per-needle SOTR for different prototypes.

Figure 30 clearly shows a per-needle SOTR of about 40 mg/hr. Also, the SOTR values are adjusted to oxygen-depleted water aeration and, at their actual DO concentration, the oxygen transfer rate is indeed lower (Figure 31). It is evident that the OTR decreases significantly as the average DO concentration increases. The reason why the actual OTR is so much lower than the calculated 55 mg/hr optimum OTR is because of the actual per-needle flow rate of the prototypes. The air flow rate used in experiments was well below 4 ml/min as was assumed in the optimum OTR calculations (Table 5). In the experiments, due to the restricted flow rates, more needles resulted in lower per-needle flow rates.

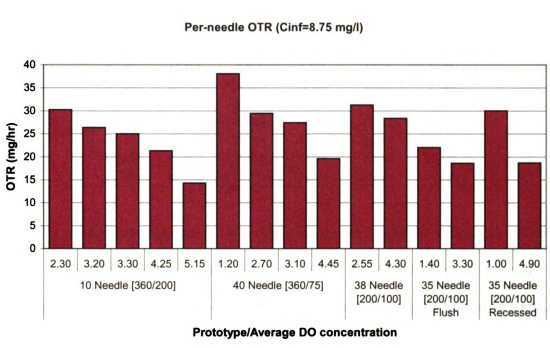

Figure 31. Per-needle OTR for different prototypes

Although the OTR do not necessarily reach 55 mg/hr, the value of 55 mg/hr for optimum OTR is fairly accurate compared to the experimental data. Increased air flow rate, and deeper submersion depth (increased OTE) could increase OTR significantly. It raises the question: if SOTR is the aerator's design's weakness, what is the practical significance of this shortcoming? Natural lake and river systems have a BOD_5 (biological oxygen demand) of at most 10 mg/L. This means that the biological oxygen demand for 5 days is 10 mg/L. For water treatment lagoons (1 acre, 7' deep), this is about 3 pounds per hour during the summer, which translates to about 18 mg/L over 5 days. This is slightly more than natural systems due to the amount of biological activity present in these lagoons. Table 7 shows the number of needles required to attain this aeration rate of 3 lb/hr for the 1-acre lagoon. A good approximation would be about 25000 needles to maintain a BOD5 of 18 mg/l which equates to an air flow rate of about 100 l/min.

Table 7. Needles required for different OTRs and BOD5s for a 1 acre, 7' deep lagoon (8634 m^3)

		per needle oxygen transferred (mg/hr)				
		25	50	55	75	100
BOD5 (mg/l)	5	14,390	7,195	6,541	4,797	3,598
	10	28,780	14,390	13,082	9,593	7,195
	15	43,170	21,585	19,623	14,390	10,793
	18	51,804	25,902	**23,547**	17,268	12,951
	20	57,560	28,780	26,164	19,187	14,390
	25	71,950	35,975	32,705	23,983	17,988
	30	86,340	43,170	39,245	28,780	21,585

The energy consumption of aeration systems will now be discussed. Table 5 shows a practical water/air flow ratio of 10-30 which means that at an air flow of 100 l/min, 1000-3000 l of water should be pumped. At the operating pressure of 22 kPa, it equates to about 0.4 to 1.1 kW (water operating pressure does not change with the depth of the aerator) of water pumping work. The small amount of air pumping work is less than 10%. Let the total pumping work (at 100% efficiency) be 0.5-1.2 kW or about 1-2 hp. The energy input seems reasonable, though, compounding inefficiencies, including pumping efficiency, motor efficiency and gear efficiency, may increase the energy requirement significantly.

The surface area of the aerator should also be taken into account. In the prototypes, needles were spaced about 5-8 mm apart. This spacing might, practically, be reduced to about 3 mm. For a square grid, 25000 needles could, theoretically fit in a 50 by 50 cm square if they're spaced this closely together. Placing the needles in this geometry would be impractical. Pumping water at 40 l/s through a plenum that small would also have adverse effects on the distribution of flow to the orifices. It is most likely that for maximum aeration, several *modules* with several hundred needles each would have to be spread out over the lagoon.

When the aeration performance of the design is compared to today's conventional aerators it is found that the design in its current stage has some minor performance advantages over conventional aerators.

Table 8. Comparison between this design and conventional aerators.

Category	This Aerator	Ceramic Fine Bubble	Fine Bubble
Bubble Size	100-400	50-500	500-3000
SAE	o/+	o	o/–
SOTR	o/–	–	o/+
OTE	+	+	o/–
Maintenance	o/–	–	o/+
Simplicity	–	o	+
Best Application	N/A	Aqua-culture and aquariums	Wastewater treatment

Bad: (–), Marginal: (o/–), Average: (o), Good: (o/+), Excellent: (+)

Gains can be made in SAE, SOTR and OTE by submerging the aerator deeper. Furthermore, simplicity and maintenance factors may be improved by better design. Possible design improvements, additional testing and additional operational requirements are discussed in the chapter on Recommendations.

4.5 Other practical considerations

There are some difficulties process and material choice of the aerator. The resiliency of the fused-silica tubing has not been tested. It is important that these tubes (or needles) hold up well in the sub-aquatic environment. The needle (or tubing) length is a minimum of 10 mm and its inside diameter is a maximum of 150 microns. This ratio may

lead to clogging issues. Although no clogging was encountered during experimental trials, it was found that during assembly, volatile glue vapors (of Loctite 404) had an affinity for the needle inner surface. This problem can be avoided by using another type of adhesive. It is also important that all needles have the same pressure drop across their length to ensure even flow rates. During experiments, 43%-74% of the needles did not produce any flow. If this occurs in practice it would reduce the SOTR by this amount and it would also reduce the SAE, but less significantly. Using another type of material for the needle is not currently practical as fused silica tubing is the only tubing with such small outer diameter (200 micron). Alternatives with slightly wider outer diameters are: PEEK capillary tubing and Teflon capillary tubing, which are available in 360 micron diameters.

Another practical problem is in the need to filter the fluids. Air filtering is not of concern, as the minimum passage diameter is 100 micron. Although the same is true for water (minimum passage diameter of 160 micron), much bigger particles may be suspended in the water and its higher viscosity inevitably leads to a higher pressure drop. Considering the operating pressure of 4-5 psi of a filter-less aerator, a filter pressure drop of the same magnitude would decrease the efficiency of the aerator by half. It is then of the greatest importance to find a suitable water filter for the aerator. Sediment filters may suffice in this application. Sediment filters are available for a wide range of flow rates (up to 5000 gph), filter size (down to 5 micron) and minimal nominal pressure drops (down to 0.1 psi), requiring only minimal extra pumping power.

In regard to the question of pumping efficiencies, both water and air are pumped at pressures of around 5 psi (3m of H_2O). Most industrial water pumps are not suited for

low pressure application while most compact submersible pumps operate at a lower pressure. It is important that, for any application, a pump operates at its maximum efficiency. It was found that some marine bilge pumps operate in the same pressure range as the aerator prototype while having a relatively large flow rate. However, even if the perfect pump was found, the shaft to work efficiency η_p (pumping efficiency) would not be much more than 0.70, while the wire to shaft efficiency η_w (electrical motor efficiency) is at most 0.95. The amended value for SAE would then become:

$$SAE_{practical} = SAE_{ideal}\eta_p\eta_w \leq 0.66SAE_{ideal} \tag{15}$$

A major advantage of the water assisted aeration technique is the increased movement of water. Advection may be considerably greater than in conventional aerators. Strategic placement of the aerators and their water intakes may produce a very favorable current in the water.

A second advantage is the fact that the aerator can be submerged deeper without major work increases. Consider the equation for total aerator work:

$$\begin{aligned} \dot{W} &= Q_{water}\Delta P_{water} + Q_{air}\Delta P_{air} \\ &= Q_{air}\left(R_Q\Delta P_{water} + \Delta P_{air,internal} + \rho_{water}gz\right) \end{aligned} \tag{16}$$

Here R_Q is the water to air flow ratio and z is the aerator depth. Since the water and air pressure are of the same order and R_Q>10 it can be observed that most of the pressure drops are internal water and air pressure losses, while the hydrostatic pressure change is relatively small. Lagoons usually have a depth of up to 10 ft (3 m). Aerator placement at this depth increases the bubble exposure to the water by at least three times compared to the experimental depth of 0.80 m.

CHAPTER 5

CONCLUSIONS

Although the success of the project depended on a practical and energy efficient new design for an aerator, its main goal was to test the viability of using a new micro-bubble generation technique for application in water aeration. Several conclusions can be made from the project:

- The micro-bubble generation technique in its original sense is a very energy efficient method of creating micro-bubbles. However its application depended on its consistency and repeatability, which was difficult to achieve in air-water systems.
- A design that made a compromise in reducing efficiency but improving consistency proved to be a viable option for implementation in an energy efficient aerator.
- The new design has several performance limitations:
    - The new design's major limitation is its total aeration capability due to a limit on the amount of air pumped through each orifice. The relative amount of air pumped is much less than standard fine bubble diffusers but similar to the fine pore ceramic diffusers, which have similar limitations.
    - Its operating pressure (4-5 psi) is higher than most aerators (2-6 psi) but much lower than ceramic fine bubble diffusers (30-45 psi).

- The per-orifice manufacturing cost is much higher than most fine bubble diffusers due to the relatively complex design.
- The per-orifice total fluid flow rate is much higher than most diffusers because of the large fraction of water pumped through the orifice.

- The new design's performance advantages over conventional aerators include:
  - The aerator can be submerged deeper with minimal energy consumption increase.
  - The aerator's fluid flow passages have a relative large minimum diameter (100 micron) compared to conventional aerators (3-100 micron) and ceramic diffusers (0.1-3 micron).
  - Simultaneous pumping of water and air increases the turn-over efficiency of aeration.
- Overall, the aerator design seems to have acceptable numbers for efficiency (SAE) and aeration (SOTR). The numbers shown for SAE in this report, however, are highly idealized, and are thus not directly practical.

CHAPTER 6

RECOMMENDATIONS

As a continuation of this project, and to obtain better understanding of the *multi-stream* aerator performance, it is recommended that:

- The aerator efficiency is tested at greater depths to obtain the maximum SAE.
- The aerator efficiency is calculated with practical pump efficiencies.
- The aerator is operated under different air and water flow rates to observe the effect it has on bubble size.
- The aerator design is tested continuously for longer periods of time in a tougher environment to test its resiliency.
- A fully functional aerator system is built to evaluate the impact of pumping and fluid filtering losses.

It would also be of interest to observe the bubble generation process in more detail and measure the effect of coalescing of bubbles and the generated bubble sizes. In the project an assumed relationship between bubble size and operating conditions was used and only approximately verified. With the new needle placement design the equation given by Ganan-Calvo and Gordillo might no longer be a useful guide.

A design that minimizes aerator size without further constricting any fluid flows should be found. Small water plenums may cause unwanted inefficiencies in the system and very large water plenums may be impractical.

Practicality should be assessed for general application and use in conjunction with alternative energy sources. Creating self-sufficient aeration units is a possibility. Solar power is the most readily available and practical technology, but wind-energy might be more cost and space efficient. Both space and cost should be taken into consideration when designing a self-sufficient aerator unit.

Pumps may be designed to specifically satisfy the need of the aerator and to maximize its efficiency under the aerator's standard operating conditions, in an effort to maximize the aeration efficiency of the aerator and to minimize its power consumption.

It is also recommended that a precision machined multi-streamed aerator functioning on the initial design as described in Chapter 1 is built. Although experiments concluded that the roughly built *single-stream* prototypes could not reliably create continuous micro-bubble generation, it was found that this was mostly due to the required precision in the placement and dimension of several parts. It should certainly be checked whether this precision can be achieved by precision machining and a more robust design. Apart from a more robust and accurately manufactured device, the fluid flows can also be controlled more precisely, reducing pressure fluctuations and making the prospect of a reliable and energy efficient aerator more likely.

APPENDICES

APPENDIX A

SOTR calculations and sources of error

Here, the various calculations and assumptions made in obtaining various aeration values are discussed. Many assumptions were made to simplify the calculations, comparisons or experiments. Starting with the calculations for SOTR, it was found that SOTR could be expressed as [14]:

$$SOTR = K_{a,20°C} \cdot C^*_{\infty,20°C} \cdot V$$

$$SOTR = K_{a,20°C} \cdot C^*_{standard,20°C} \left(\frac{(1+d_e/10.24)P_{atm} - P_{sat}}{P_{atm} - P_{sat}} \right) \cdot V \tag{17}$$

$$SOTR = K_{a,20°C} \cdot C^*_{standard} \left(\frac{31.6+T}{51.6} \right) \left(\frac{(1+d_e/10.24)P_{atm} - P_{sat}}{P_{atm} - P_{sat}} \right) \cdot V$$

where the temperature is in degrees Celsius and the pressure in kPa. For the experiments, the pressure correction is ignored because its variations are negligible ($P \approx P_{atm} = 101 kpa$). The temperature correction is retained, because these results are more sensitive to it. Over the temperature range of $19.2°C \le T \le 23.4°C$, the SOTR varies by 8%. But K_a can be approximated and the equation for SOTR becomes:

$$SOTR = \left. \frac{dC(t)}{dt} \right|_t \frac{C_\infty}{C_\infty - C(t)} \cdot V = \frac{(C_2 - C_1)}{(t_2 - t_1)} \frac{C_\infty}{C_\infty - \left(\frac{C_2 + C_1}{2} \right)} \cdot V \tag{18}$$

Analysis of this approximation shows that as $C \to C_\infty$, it will amplify the uncertainty in C_∞. Furthermore, when $C_2 >> C_1$, SOTR will be underestimated compared to the actual value for SOTR. Since, for all the experimental trials $C_2 < 5\frac{mg}{l} << C_\infty$ a constant value for C_∞ was used for every trial. The value that was

used was 8.75 mg/l, which accommodated the slightly higher temperatures and minimal salinity. Then the value for SOTR was obtained using:

$$SOTR = \frac{\Delta C}{\Delta t} \frac{8.75}{8.75 - C_{av}} \cdot V \tag{19}$$

The only issue now is to find ΔC/Δt. These values were simply approximated from data graphs Figure 32.

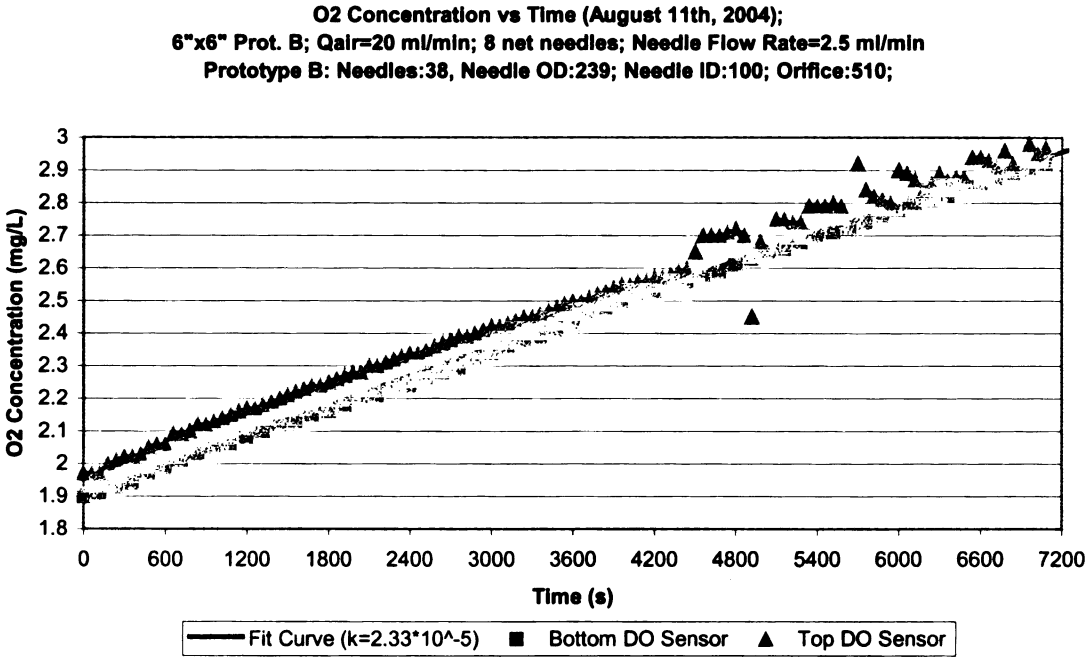

Figure 32. Example graph for finding the values for calculating SOTR.

Using Excel, a linear fit (not shown) could be applied from which the average slope was obtained. Using the slope the values for K_a and SOTR were calculated. These values were verified by applying a manual fit using the equation: $C(t) = C_\infty \left(1 - e^{K_a (t - t_0)}\right)$, for which $C_\infty = 8.75 \frac{mg}{l}$. K_a was obtained using this approximation and t_0 was guessed and visually verified on the graph (red line).

In this project $C_{\infty} = 8.75 \frac{mg}{l}$ for multi-stream aerators and $C_{\infty} = 9.00 \frac{mg}{l}$ for single stream aerators. So, how much does this affect the accuracy of the SOTR if the actual value for C_{∞} is different. From Figure 33 it can be observed that when $C_{av} < 5.00 \frac{mg}{l}$ and $8.50 \frac{mg}{l} \leq C_{\infty,actual} \leq 9.00 \frac{mg}{l}$, there is an error in SOTR of less than ±5%. It can also be observed that for small values of C_{av}, the actual value of C_{∞} has very little effect on SOTR.

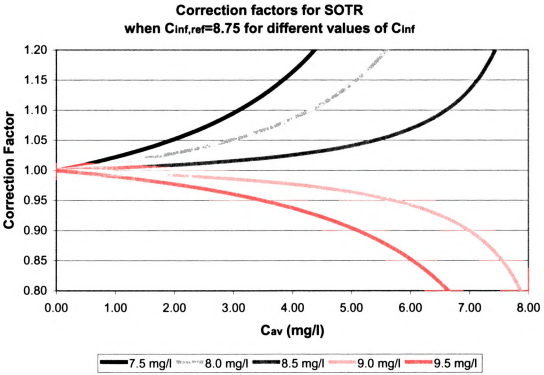

Figure 33. Correction factors for SOTR for variations in C_{inf}.

The correction factor can be obtained using the following relation.

$$corr. = \left(\frac{C_{\infty,ref}}{C_{\infty,act}}\right)\left(\frac{C_{\infty,act} - C_{av}}{C_{\infty,ref} - C_{av}}\right) = \left(\frac{8.75}{C_{\infty,act}}\right)\left(\frac{C_{\infty,act} - C_{av}}{8.75 - C_{av}}\right) \tag{20}$$

Consequently, the effect of this correction can be applied to the calculations for SAE. Table 9 shows the variation in SAE for different values of $C_{\infty,actual}$. It clearly shows that underestimating C_{∞} results in overestimating SAE and overestimating C_{∞} results in underestimating SAE. For example, if the actual value for C_{∞} was 8 mg/l then the last prototype would have an average SAE of 5.06, not 4.70 as listed in Table 6. (Remember, C_{∞} was estimated to be 8.75 mg/l).

Table 9. Variation of SAE for different values of $C_{\infty,actual}$.

	Average SAE for different actual C_{inf}				
Prototype	C_{inf}=8 lb/hp-hr	C_{inf}=8.5 lb/hp-hr	C_{inf}=8.75 lb/hp-hr	C_{inf}=9 lb/hp-hr	C_{inf}=9.5 lb/hp-hr
10 Needle [360/200]	3.16	2.99	2.94	2.87	2.76
40 Needle [360/75]	4.59	4.45	4.39	4.32	4.22
38 Needle [200/100]	4.01	3.81	3.75	3.66	3.53
35 Needle [200100] Flush	3.47	3.38	3.34	3.30	3.23
35 Needle [200100] Recessed	5.06	4.79	4.70	4.58	4.42

APPENDIX B

Theoretical aeration efficiency calculations

The aeration of water is roughly proportional to the contact surface area between water and air.

$$Aeration = k_L A_{surface} = k_L 6 \frac{Q_{air}}{D_{bubble}} \Delta t \tag{21}$$

It was assumed that the bubble diameter is a function of the fluid flow rates and the orifice diameter.

$$D_{bubble} = D_{orifice} \left(\frac{Q_{air}}{Q_{water}} \right)^{0.37} = D_{orifice} \left(R_Q \right)^{-0.37} \tag{22}$$

Lastly, the work input can be defined as:

$$\dot{W} = Q_{air} \left(R_Q \Delta P_{water} + \Delta P_{air,internal} + \rho_{water} g z \right) \tag{23}$$

where the pressure drop of water through the orifice is calculated as if it were a flow between parallel plates a distance r_o-r_i apart [15]:

$$\Delta P_{water} = \left(\frac{dP_w}{dx} \right) \Delta x = \left(\frac{12 \mu_w}{(r_o - r_i)^2} \frac{Q_w}{\pi (r_o^2 - r_i^2)} \right) z_{orifice} \tag{24}$$

Here it is assumed that the pressure drop through the orifice is much larger than any other pressure drop in the system. Similarly the pressure drop of air can be calculated by calculating the pressure drop across the air feeding needle and assuming that this pressure drop is much larger than any other in the system:

$$\Delta P_{air} = \left(\frac{8 \mu_a}{r_{needle}^2} \frac{Q_a}{\pi r_{needle}^2} \right) z_{needle} + \rho_w g z_w < \Delta P_{water} \tag{25}$$

It was found that this theoretical air pressure is less than the water pressure for a depth of 0.80 m in these experiments. For larger depth, it can also be found that:

$$\left(\frac{8\mu_a}{r_{needle}^2}\frac{Q_a}{\pi r_{needle}^2}\right)z_{needle} << \rho_w g z_w \approx \Delta P_a \tag{26}$$

The equation for work can then be simplified to:

$$\dot{W} = Q_a\left(\left(R_Q + \frac{\Delta P_a}{\Delta P_w}\right)\Delta P_w\right) = Q_a\left(\left(R_Q + \frac{1}{R_P}\right)\Delta P_w\right) \tag{27}$$

and substituting:

$$Aeration = k_L 6\frac{Q_a}{D_{orifice}\left(R_Q\right)^{-0.37}}\Delta t \tag{28}$$

The aeration efficiency is defined as the aeration divided by the work input:

$$SAE \sim \frac{Aeration}{Work} = \frac{k_L 6\left(R_Q\right)^{0.37}}{D_{orifice}\left(\left(R_Q + \frac{1}{R_P}\right)\left(\frac{12\mu_w}{(r_o - r_i)^2}\frac{Q_w}{\pi(r_o^2 - r_i^2)}\right)z_{orifice}\right)} \tag{29}$$

Let $R_Q >> 1/R_P$, the equation then simplifies to:

$$SAE \sim k_L\left(\frac{\pi(d_o^2 - d_i^2)(d_o - d_i)^2}{32\mu_w d_o z_{orifice}}\right)\left(\frac{Q_a^{0.63}}{Q_w^{1.63}}\right) \tag{30}$$

If there are other major water pressure drops present and those pressures are relative to the rate of water flow then:

$$SAE \sim k_L\left(\frac{32\mu_w d_o z_{orifice}}{\pi(d_o^2 - d_i^2)(d_o - d_i)^2} + f\right)^{-1}\left(\frac{Q_a^{0.63}}{Q_w^{1.63}}\right) \tag{31}$$

where $P = f \cdot Q_w$. This allows for the theoretical analysis of the water and air flow rates' effect on the SAE. It is then obvious, with the pressure term being constant, that for

maximum SAE, a minimum water flow rate and a maximum air flow rate are desired. Because a minimum water to air ratio is required, as was discussed earlier on, it is also evident that a minimum total flow rate is desired for the greatest SAE. However, a minimum total flow rate results in a minimum SOTR. The challenge is then to create the lowest water to air flow rate ratio that avoids coalescence of bubbles.

APPENDIX C

Micro-bubble size measurements (single stream prototypes)

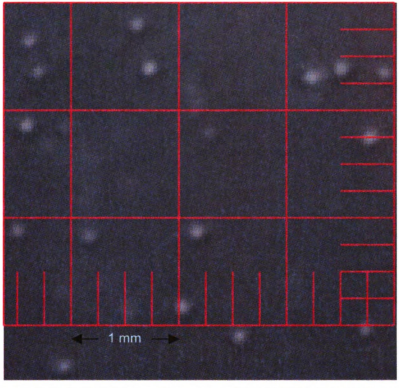

$h \approx 11$ mm
$D_{bubble} \approx 180\text{-}250$ µm
$Q_{water} = 5$ ml/min
$Q_{air} = 0.5$ ml/min
$D_{Orifice} \approx 450$ µm
$H_{Orifice} \approx 150$ µm
$P_{hydro} \approx 10.0$ kPA

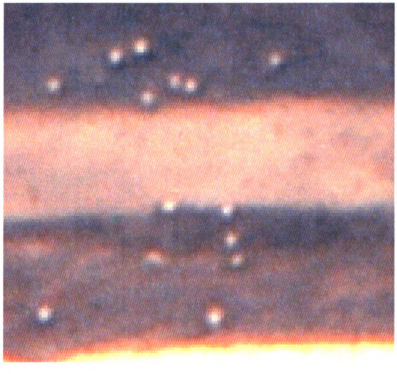

$h \approx 2$ mm
$D_{bubble} \approx 180\text{-}250$ µm
$Q_{water} = 5$ ml/min
$Q_{air} = 0.5$ ml/min
$D_{Orifice} \approx 450$ µm
$H_{Orifice} \approx 150$ µm
$P_{hydro} \approx 10.0$ kPA

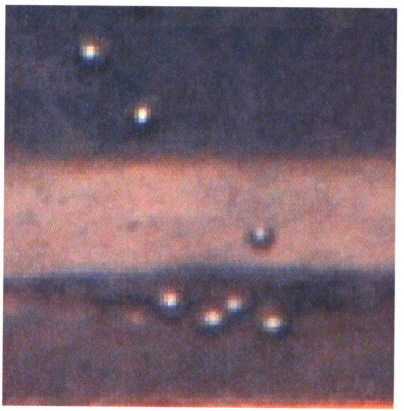

$h \approx 2$ mm
$D_{bubble} \approx 250\text{-}300$ µm
$Q_{water} = 5$ ml/min
$Q_{air} = 0.5$ ml/min
$D_{Orifice} \approx 450$ µm
$H_{Orifice} \approx 150$ µm
$P_{hydro} \approx 10.0$ kPA

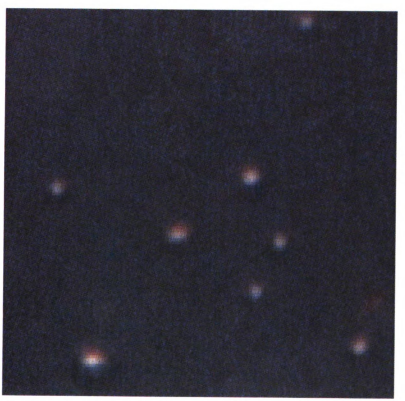

$h \approx 4$ mm
$D_{bubble} \approx 200\text{-}270$ µm
$Q_{water} = 5$ ml/min
$Q_{air} = 0.5$ ml/min
$D_{Orifice} \approx 450$ µm
$H_{Orifice} \approx 150$ µm
$P_{hydro} \approx 10.0$ kPA

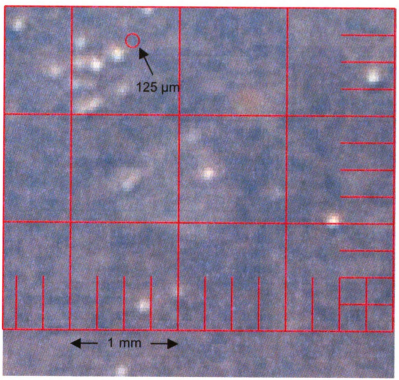

h ≈ 3 mm
D_{bubble} ≈ 170-230 µm
Q_{water} = 5 ml/min
Q_{air} = 0.5 ml/min
$D_{Orifice}$ ≈ 450 µm
$H_{Orifice}$ ≈ 150 µm
P_{hydro} ≈ 10.0 kPA

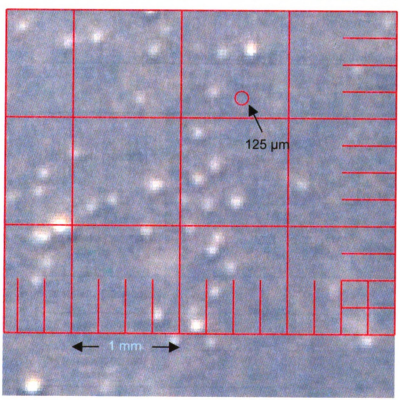

h ≈ 5 mm
D_{bubble} ≈ 150-250 µm
Q_{water} = 5 ml/min
Q_{air} = 0.5 ml/min
$D_{Orifice}$ ≈ 450 µm
$H_{Orifice}$ ≈ 150 µm
P_{hydro} ≈ 10.0 kPA

APPENDIX D

Prototype data (multistream prototypes)

Table 10. Prototype operating conditions

Prototype	C(avg)	Theoretical Pressure	Measured Pressure	Water Flow Rate	Water Pumping Work	Air Flow Rate
	mg/l	Pa	Pa	l/min	W	ml/min
10 Needle [360/200]	2.30	26,018	2,7440	0.50	0.23	20.00
	3.20	26,018	27,440	0.50	0.23	20.00
	3.30	26,018	27,440	0.50	0.23	20.00
	4.25	26,018	27,440	0.50	0.23	20.00
	5.15	26,018	27,440	0.50	0.23	20.00
40 Needle [360/75]	1.20	20,814	24,500	1.60	0.65	45.00
	2.70	20,814	24,500	1.60	0.65	45.00
	3.10	20,814	24,500	1.60	0.65	45.00
	4.45	20,814	24,500	1.60	0.65	45.00
38 Needle [200/100]	2.55	5,997	26,460	1.94	0.86	20.00
	4.30	5,997	26,460	1.94	0.86	20.00
35 Needle [200/100] Flush	1.40	5,016	21,070	1.41	0.50	30.00
	3.30	5,016	21,070	1.41	0.50	30.00
35 Needle [200/100] Recessed	1.00	5,230	19,600	1.47	0.48	40.00
	4.90	5,230	19,600	1.47	0.48	40.00

Table 11. Prototype operating conditions

	Net Needles	Total Needles	Needle ID	Needle Length	Submerged Depth	Adjustment Factor
	#	#	micron	mm	m	#
10 Needle [360/200]	5	10	200	10	0.80	0.50
	5	10	200	10	0.80	0.50
	5	10	200	10	0.80	0.50
	5	10	200	10	0.80	0.50
	5	10	200	10	0.80	0.50
40 Needle [360/75]	16	40	75	10	0.80	0.40
	16	40	75	10	0.80	0.40
	16	40	75	10	0.80	0.40
	16	40	75	10	0.80	0.40
38 Needle [200/100]	10	38	100	15	0.80	0.26
	10	38	100	15	0.80	0.26
35 Needle [200/100] Flush	20	35	100	15	0.80	0.57
	20	35	100	15	0.80	0.57
35 Needle [200/100] Recessed	20	35	100	14	0.80	0.57
	20	35	100	14	0.80	0.57

Table 12. Prototype/Trial k values and related properties

Prototype	dC/dT	C Avg.	k		k (per stream)	
		mg/L	1/s (x10^-6)	1/hr	1/s (x10^-6)	1/hr
10 Needle [360/200]	0.000070	2.30	10.85	0.0391	2.17	0.0078
	0.000061	3.20	10.99	0.0396	2.20	0.0079
	0.000058	3.30	10.62	0.0382	2.12	0.0076
	0.000049	4.25	10.96	0.0394	2.19	0.0079
	0.000033	5.15	9.17	0.0330	1.83	0.0066
40 Needle [360/75]	0.000282	1.20	37.32	0.1344	2.33	0.0084
	0.000218	2.70	36.05	0.1298	2.25	0.0081
	0.000203	3.10	35.93	0.1293	2.25	0.0081
	0.000145	4.45	33.71	0.1214	2.11	0.0076
38 Needle [200/100]	0.000145	2.55	23.34	0.0840	2.33	0.0084
	0.000131	4.30	29.51	0.1062	2.95	0.0106
35 Needle [200/100] Flush	0.000204	1.40	27.74	0.0998	1.39	0.0050
	0.000172	3.30	31.60	0.1138	1.58	0.0057
35 Needle [200/100] Recessed	0.000278	1.00	35.84	0.1290	1.79	0.0065
	0.000173	4.90	44.90	0.1616	2.24	0.0081

Table 13. Prototype/Trial SOTR values

Prototype	SOTR			per stream SOTR		
	lb/hr	mg/s	mg/hr	lb/hr (x10^-6)	mg/s	mg/hr
10 Needle [360/200]	0.000451	0.0570	205	90.3	0.01140	41.02
	0.000457	0.0577	208	91.4	0.01154	41.55
	0.000442	0.0558	201	88.3	0.01116	40.16
	0.000456	0.0575	207	91.1	0.01150	41.41
	0.000381	0.0481	173	76.2	0.00963	34.65
40 Needle [360/75]	0.001552	0.1959	705	97.0	0.01225	44.09
	0.001499	0.1893	681	93.7	0.01183	42.59
	0.001494	0.1886	679	93.4	0.01179	42.44
	0.001402	0.1770	637	87.6	0.01106	39.82
38 Needle [200/100]	0.000971	0.1225	441	97.1	0.01225	44.11
	0.001227	0.1549	558	122.7	0.01549	55.77
35 Needle [200/100] Flush	0.001153	0.1456	524	57.7	0.00728	26.21
	0.001314	0.1659	597	65.7	0.00830	29.87
35 Needle [200/100] Recessed	0.001490	0.1882	677	74.5	0.00941	33.87
	0.001867	0.2357	849	93.3	0.01179	42.43

Table 14. Prototype/Trial SAE, OTE, R_Q and OTR values

Prototype	Adjusted SAE			OTE	R_Q	Per Needle OTR
	lb/HPhr	kg/kw hr	kg/kj	%		mg/hr
10 Needle [360/200]	3.02	1.79	0.50	47.6	12.50	30.24
	3.06	1.82	0.50	41.5	12.50	26.35
	2.96	1.76	0.49	39.3	12.50	25.01
	3.05	1.81	0.50	33.5	12.50	21.30
	2.55	1.52	0.42	22.4	12.50	14.26
40 Needle [360/75]	4.54	2.70	0.75	85.1	14.22	38.04
	4.39	2.61	0.72	65.9	14.22	29.45
	4.37	2.60	0.72	61.3	14.22	27.40
	4.10	2.44	0.68	43.8	14.22	19.57
38 Needle [200/100]	3.30	1.96	0.54	98.3	25.53	31.26
	4.17	2.48	0.69	89.2	25.53	28.36
35 Needle [200/100] Flush	3.12	1.85	0.51	92.4	26.86	22.02
	3.55	2.11	0.59	78.0	26.86	18.60
35 Needle [200/100] Recessed	4.15	2.47	0.69	94.4	21.00	30.00
	5.20	3.09	0.86	58.7	21.00	18.67

REFERENCES

1 U.S. Environmental Protection Agency, "Wastewater technology fact sheet: aerated, partial mix lagoons," EPA 832-F-02-008, 2002, Washington DC

2 Gordillo, J. M., Ganan-Calvo, A. M. and Perez-Saborid, M., "Monodisperse microbubbling: Absolute instabilities in co-flowing gas-liquid jets", In *Physical of Fluids, Vol 13, # 12*, The American Institute of Physics, December 2001

3 Forday, W. L, "Biomechanical engineering: frequently asked questions," http://www.np.edu.sg/~dept-bio/bce_faq/biochemical_engineering_mass_transfer.htm

4 Hitchman, M. L., "Measurement of Dissolved Oxygen", pp 7-32, John Wiley & Sons, 1978

5 Motarjemi, M. and Jameson, G. J., "Mass transfer from very small bubbles-the optimum bubble size for aeration", Chemical Engineering Science, Vol. 33, pp 1415-1423, Pergamon Press Ltd., 1978

6 U.S. Environmental Protection Agency, "EPA On-line Tools for Site Assessment Calculation," http://www.epa.gov/athens/learn2model/part-two/onsite/henryslaw.htm

7 Ahmed, T. and Semmens, M. J., "Gas transfer from small spherical bubbles in natural and industrial systems", J. Environmental Systems, Vol 29(2), Baywood Publishing Co., Inc. 2003

8 Jensen, G. L., Bankston, J. D. and Jensen, J. W., "Types and uses of aeration equipment", Oklahoma Cooperative Extension Service, Oklahoma State University

9 Boyd, C.E., "Types of Aeration and Design Considerations", Department of Fisheries and Allied Aquacultures, Auburn University, Auburn, Alabama

10 Ganan-Calvo, A. M. and Gordillo, J. M., "Perfectly Monodisperse Microbubbling by Capillary Flow Focusing", In *Physical Review Letters, Vol 87, # 21*, The American Physical Society, 2001

11 U.S. Environmental Protection Agency, "Wastewater technology fact sheet: fine bubble aeration," EPA 832-F-99-065, 1999, Washington DC

12 Gordillo, J. M., Cheng, Z., Ganan-Calvo, A. M., Marquez, M. and Weitz, D. A., "A new device for the generation of micobubbles", In *Physical of Fluids, Vol 16, # 8*, The American Institute of Physics, August 2004

13 Stenstrom, M. K., "Motion of bubbles and bubble characteristics," lecture notes, University of California Los Angeles, Department of Civil and Environmental Engineering.

14 EnviroSim Associates ltd, "Aeration Calculations, basic model for oxygen transfer," 2003, http://www.envirosim.com/products/bw32/bw32kb/17_AirExam.php

15 White, F., "Fluid Mechanics", Viscous flow in ducts, pp. 327-329, McGraw-Hill, 1986